Modeling, Identification and Control, Vol. 45, No. 4, 2024, pp. 147–173, ISSN 1890–1328

Cost-Optimal Fuel Utilization, Genset Configuration and Battery Sizing: A Case-Study of a Norwegian Trawler

T. Hennum [1] Ø.K. Kjerstad [1] A.R. Nerheim [1]

[1] *Department of Ocean Operations and Civil Engineering, Norwegian University of Science and Technology, N-6009 Ålesund, Norway. E-mail: {tor.hennum, oivind.k.kjerstad, ann.r.nerheim}@ntnu.no*

Abstract

The energy transition of the Norwegian ocean-going fishing fleet is challenging since there are few widely available fuel alternatives. Many large fishing vessels stay at sea for long periods between each fuelling. To complete its tasks and have space for the caught fish, an energy system which efficiently utilizes its fuel is required. This work proposes a flexible optimization-based mixed-integer linear programming tool for sizing, scheduling and analysing maritime energy systems consisting of diesel gensets and batteries, which considers both part-load engine efficiency and battery degradation. The tool is applied on a 24-hour data selection from an existing trawler, and the results point to the main fuel savings being enabled by splitting the installed power capacity into smaller gensets that can run independently from each other, and from utilizing a battery system to both reduce the total installed genset capacity to increase their relative loading and by delaying the startup of new gensets. Smaller fuel savings can be achieved from peak shaving of already running gensets. The current application achieves a 7.3 % fuel reduction in a cost-efficient manner over the period. It also suggests that a fuel-reducing system might not necessarily be cost-efficient, particularly for energy systems with small batteries.

Keywords: Fuel efficiency, Emissions reduction, Maritime energy systems, Mixed-integer linear programming, Optimization

Sub- and superscripts

0	initial/original value(s)
B	battery
c	charge
CO	continuous
CO_2	carbon dioxide
Cu	curtailment
cy	cycle
D	degradation
d	discharge
F	fuel
G	genset
I	investment/installation
L	load or lifetime
M	maintenance
m	mechanic
N	nominal
NG	number of gensets
Pr	propeller
PWA	piece-wise affine
R	running
RL	running life
rr	ramp rate
Sd	shutdown
sh	shelf
Su	startup
t	time

doi:10.4173/mic.2024.4.4

Symbols

η	%	Efficiency
ρ	kg/L	Volumetric density
Δt	h	Time resolution
Δp	–	Power ramping
b	–	PWA discretization bin indicator
C	NOK	Cost
c	*various*	Price
D	–	Battery degradation
d	–	Point in battery degradation curve
E	kWh	Energy capacity
e	MJ/kg	Gravimetric Energy density
g	–	Generator index
i_t	–	Time index
J	MNOK	Cost function
j	–	PWA discretization index
k_B	–	Degradation model parameter
$k^{\mathrm{CO_2}}$	$\mathrm{t_{CO_2}/t_{fuel}}$	Emissions intensity
V	$\mathrm{m^3}$	Fuel consumption
$\dot{V}$	$\mathrm{m^3/h}$	Fuel volume rate
$\dot{m}$	kg/h	Fuel mass rate
$\bar{m}$	$\mathrm{kg_F/MWh}$	BSFC/PSFC curve
N	–	Number of something
$\dot{n}_\mathrm{B}$	$\mathrm{h^{-1}}$	Battery C-rate
P, p	W, –	Power
$\dot{p}$	%/min	Power ramp rate
q_SoC	–, %	State of charge
T	h, yrs	Expected life time
w	–	PWA discretization index weight
z	–	Boolean indicator/signal

1 Introduction

Sustainable access to nutritious food is important to feed a growing world population (United Nations (2021)). Health agencies in the EU and Norway recommend the population eat fish every week (European Commission (2024); Norwegian Directorate of Health (2024)) and the Norwegian fishing industry is heavily regulated to be sustainable (Norwegian Seafood Council (2020)). However, the Norwegian fishing industry is still mainly run on fossil fuels. Both the International Maritime Organization (IMO) and the Norwegian Government have committed to cutting greenhouse gas emissions over the next decades and as a part of the maritime sector, the fishing industry is under increasing political pressure to reduce its climate gas emissions.

The Norwegian fishing fleet consists of a large variety of different vessels with a large size range, fishing equipment and operational patterns. The trawler is a vessel type with power- and energy-demanding equipment that catches large volumes of fish per trip and, due to long stays at sea requires a dense energy system (Norwegian Directorate of Fisheries (2024)). The term "energy system" refers to systems consisting of both power-generating and energy-storing components, such as generator sets (gensets) and batteries.

A large part of the emissions from the fishing sector is from fuel consumption (Norges Fiskarlag (2020)). No sustainable fuel alternatives are energy-dense enough, mature enough and available enough at scale to replace the currently used marine gas/diesel oil yet. This makes improvements in fuel-efficiency one of the most important steps which can be done over the upcoming few years.

The Norwegian governmental institution Enova has historically given financial support to ship companies for installing batteries and energy efficiency measures, and is currently working on developing new support programs for electrification in the maritime sector (Enova (2024)).

Which energy system a ship owner chooses is typically dependent on what is cost-efficient, but at the same time, many ship owners search for ways to cut emissions. They have few incentives to cut emissions other than costs, which are heavily impacted by the investment, maintenance and operational costs of different technologies, which can both be subsidised and taxed by authorities depending on the desired trajectory of development. Price levels, as well as carbon taxes and similar political instruments, do, however, change over time, making it less predictable for the ship owners in terms of what they should invest in.

Input from several ship owners is that they do not really see the need for implementing batteries onboard their vessels and that they would not have invested in it without governmental support. System analysis, which provides knowledge about the actual cost savings potential from implementing a battery and how large its capacity should be, could help the design companies to give credible advice to the ship companies and accelerate a widespread implementation. Knowledge about which types of vessels have a high potential could further be of interest to the governmental side to ensure that the economic support is used where it has the largest impact.

For this reason, it is interesting to have a tool available that can be used to investigate how to size gensets and batteries for both new systems and retrofits and, furthermore, be used to utilize the already existing systems optimally. The tool should not be so complex that it becomes unrealistic to implement and should not grow so large that it becomes numerically unrealistic to include necessary operational constraints.

The power management of a maritime vessel is a multi-objective task. The power demand must be met at all times, the fuel consumption should be limited, the degradation of the battery should be limited, and

the running hours of the engines/gensets should be kept to a minimum. However, frequent starting and stopping and rapid ramping of the power units should also be avoided to limit the stress on the equipment and the need for maintenance. For the purpose of making an optimization problem which considers installing gensets or not, when to run them as well as including certain non-linear phenomenons, mixed-integer linear programming (MILP) algorithms using linearized piece-wise affine functions show promise.

Focusing on limiting emissions through efficient utilization of the energy systems in the maritime sector is not new. There has been suggested different optimization approaches to design, control and analyse energy systems to achieve emissions reductions. One example is Vieira et al. (2022), who investigated the possible fuel emissions reductions of a platform supply vessel. However, they set most costs to zero in order to investigate the maximum potential fuel savings regardless of price. They also used proprietary and licenced software to run the analysis.

Skjong et al. (2017) suggested a MILP-based approach to consider different important objectives and aspects. They looked into different vessels, but not fishing vessels. Furthermore, they kept the number of gensets to a fixed number. This work used multi-objective cost functions where power balance, starting/stopping and number of running hours were weighed together using tuned parameters, and a minimum genset power constraint was not included in the MILP problem itself. It took into account an assumed optimal loading but not the fuel curve itself.

Another example is the study by Marocco et al. (2021), which investigated the design of renewable battery-hydrogen energy systems using a MILP framework. One focus of this algorithm is the design of the battery system, but it does not use traditional gensets and was run with a low time resolution of one hour.

Wang et al. (2016) presented an alternative for implementing a linearized degradation model for a battery in the MILP optimization problem, where frequent and unhealthy usage of the battery is penalized through a cost for the degradation.

Expanding the analysis and battery sizing by including different scenarios is possible. These scenarios can be generated using various load forecasting models or based on input from the crew, depending on the planned activities. An alternative is to use a data-driven approach, such as the one suggested by Chapaloglou et al. (2022), using load forecasting, such as the one suggested by Chapaloglou et al. (2019). However, this grows the model drastically in size.

Contributions and Objectives

This work aims to develop and document a functioning optimization-based approach to achieve realistic emissions reductions for a Norwegian trawler and purse seiner, with the motivation of the ship owner and operator in mind. The main contribution of this work is an alternative approach to designing maritime energy systems, which the industry can adopt when planning their next steps of addressing emissions reductions in the maritime sector. It is possible to set up independently of specific software and solvers and it is most relevant for ship designers to better advise ship companies which system configuration and operational pattern they should go for.

This article presents a single-objective MILP approach to limit emissions from ships. This is achieved by minimizing the overall system cost through optimizing the system configuration and utilization. The approach investigates realistic emissions reductions from a system cost perspective instead of the theoretical maximum reduction while avoiding certain impractical system operations. The optimization scheme can be applied to any isolated energy system consisting of gensets, energy storage and power loads. Still, the focus of the current work is developing a flexible tool for fishing vessels.

The optimization problem considers both part-load engine fuel efficiency, battery losses and usage-related battery degradation. The penalization included in the cost function is calculated based on real costs instead of using trial and error-based tuning of weights. One result of the optimization is the optimal genset configuration based on a user-defined total power load time series and battery size, as well as time series for the resulting power flow in the system over the optimization horizon.

The optimization problem is formulated to be flexible in terms of fuel technology and battery technology by using genset fuel models and battery degradation models in generic formats. This makes it suitable for investigating the gradual steps from more optimal utilization of existing systems with and without added batteries to cost-optimal retrofitting of the system by replacing one or more gensets, to finally finding cost-optimal alternatives for new-builds with its fuel and emissions saving potential.

2 Methods

This section presents the system model and methods used for this work and their associated assumptions and limitations. An optimization scheme is presented, which aims to limit the total system cost by

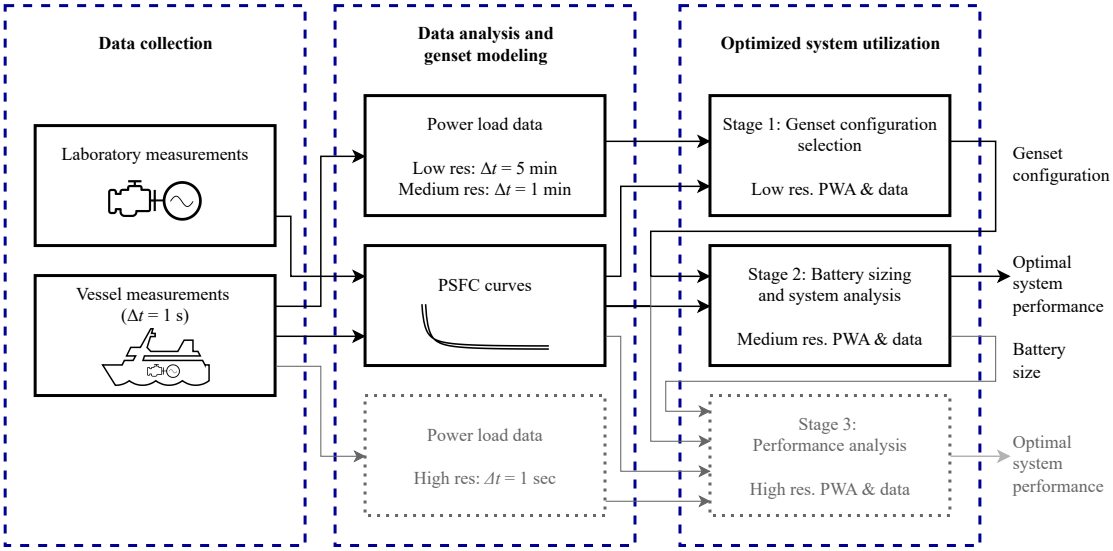

Figure 1: Overview of the collected data from the vessel and its usage. The grey area is planned future testing and validation of the output of the optimization, and is out of the scope of this work.

only installing the most cost-efficient combination of gensets and battery, through optimized utilization of the equipment by functioning as an optimization-based power/energy-management system (PMS/EMS). Fuel-efficiency and battery degradation are weighed against each other using estimates for their real costs. .

Fig. 1 illustrates the main work flow of the research. Mechanic and electric power measurements are collected from engines and generators in operation both on shore and on a fishing vessel, together with their respective fuel consumption measurements. These measurements form the basis of the work, where they are both used to make fuel consumption models and used as representative power load time series for further investigation.

The optimization tool is flexible dependent on the input, and is here suggested to be used in the two first stages found in Fig. 1. Stage 1 is a genset configuration selection stage, and Stage 2 is a battery sizing and analysis stage. A large selection of different gensets are included in Stage 1, where their sizes, types and count is dependent on the problem at hand. In order to limit the computational effort, the resolution of the models and data used is reduced. Results from this stage is used to select which gensets should be included further.

Only the chosen gensets from Stage 1 are included in Stage 2. The resolution of the models and data are now increased, in order to get more precise results. Results from the second optimization stage can then be run through a simulation framework with the same time resolution as the original measurement data, in order to further investigate the system performance compared to the existing system, as indicated in Fig. 1. This last stage is, however, outside of the scope of this article.

The energy system of the existing fishing vessel from which measurements are collected and used is presented in Sec. 2.1. The suggested alternative energy system is introduced in Sec. 2.2, together with the related optimization problem. The investigative approach is presented in Sec. 2.3 together with the parameter values and input data which were used.

Limitations

The load is based on a time series from a limited period of operation of one vessel and is set as fixed, without options to adjust the speed or shed load if necessary. Precision in the predicted power load is outside the scope of this analysis, and estimates of the total load is instead found from measurements from an existing trawler. The analysis is currently limited to systems powered by diesel-fueled gensets and a battery energy storage system.

2.1 Power Load Data for the Case Study

SINTEF Ocean has provided measurements from a fishing vessel currently in operation – a Norwegian pelagic trawler/purse seiner. These measurements have previously been used by Hennum et al. (2023), and the same pre-processing of the data was done here before further analysis.

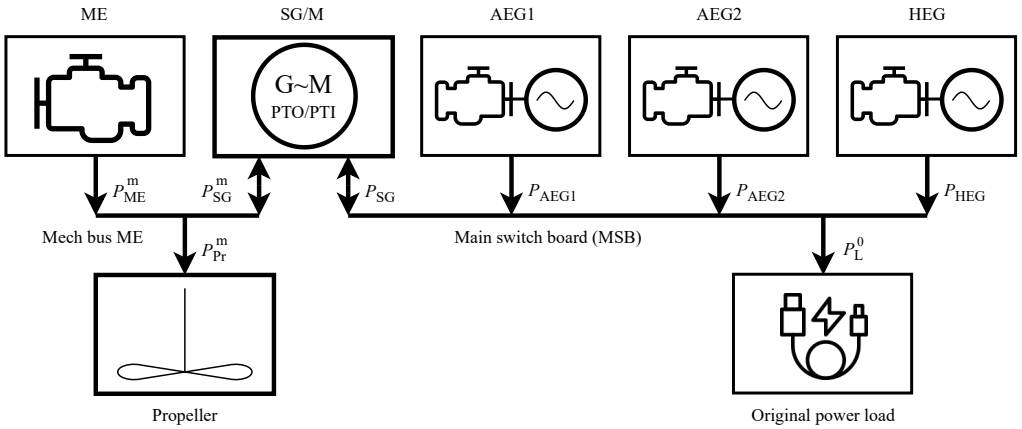

Figure 2: Illustration of the energy system of the existing vessel, with connected components and power balance.

Fig. 2 illustrates the on-board power system of the existing vessel which has four generators: one shaft generator (SG) connected to the main engine (ME), two generators in the auxiliary gensets (AEG) and one harbor/emergency genset (HEG). The electric power from the generators was measured directly. The main engine is, however, mechanically connected to the propeller, such that the mechanic input power to the shaft generator does not correspond directly to the output mechanic power of the main engine.

The original electric power consumption (P^0_{L}) in each time step (i_t) is estimated from the total measured electric power production, as seen in Eq. (1).

$$P^0_{\mathrm{L}}[i_{\mathrm{t}}] = P_{\mathrm{SG}}[i_{\mathrm{t}}] + P_{\mathrm{AEG1}}[i_{\mathrm{t}}] + P_{\mathrm{AEG2}}[i_{\mathrm{t}}] + P_{\mathrm{HEG}}[i_{\mathrm{t}}] \quad (1)$$

The objective is to evaluate the performance of distributing the load differently than currently done, and how the optimization tool works. In order to avoid varying results arising from inaccuracies in the fuel models, the collected fuel measurements are not used for comparison with the suggested system. Instead, the fuel consumption was estimated from power values and the same fuel models as the optimized system. This way, the performance of the suggested optimization scheme could be evaluated more directly. This was done using the break-specific fuel consumption (BSFC) and the power-specific fuel consumption (PSFC) models produced from the ship for the ME and AEG1/AEG2 data, respectively. The precision of using the fuel curves on the collected data is outside the scope of this article, but was addressed in Hennum et al. (2023). There were not enough data points over the whole loading range to make a full model based on the HEG data, so here the PSFC model from experimental results in a hybrid lab was used instead.

In the existing system, the main engine drives both a propeller and a shaft generator. The suggested system presented in Sec. 2.2 has no such mechanical link to the propeller. The mechanic propeller load is, for this reason, replaced by an electric load by introducing an electric motor between the electric bus and the propeller. The mechanic propeller power ($P^{\mathrm{m}}_{\mathrm{Pr}}$) was not measured, but was estimated from the difference between the mechanic SG load ($P^{\mathrm{m}}_{\mathrm{SG}}$) and mechanic ME load ($P^{\mathrm{m}}_{\mathrm{ME}}$). The equivalent electric power P_{Pr} was then calculated from Eq. (2a), using the aforementioned power difference and a constant motor efficiency (η_{M}). This increases the total power load used in Eq. (3a) with an equivalent load P_{Pr}, as seen in Eq. (2b), from P^0_{L} to P_{L}.This is used as the baseline power consumption for comparison with the optimized power flow.

$$P_{\mathrm{Pr}}[i_{\mathrm{t}}] = \frac{P^{\mathrm{m}}_{\mathrm{ME}}[i_{\mathrm{t}}] - P^{\mathrm{m}}_{\mathrm{SG}}[i_{\mathrm{t}}]}{\eta_{\mathrm{M}}} \quad (2a)$$

$$P_{\mathrm{L}}[i_{\mathrm{t}}] = P^0_{\mathrm{L}}[i_{\mathrm{t}}] + P_{\mathrm{Pr}}[i_{\mathrm{t}}] \quad (2b)$$

The mechanic SG power ($P^{\mathrm{m}}_{\mathrm{SG}}$) was not measured, but instead estimated from the measured electric power P_{SG} and efficiency models for the shaft generator, under the assumption that it has the same part-load properties as the two generators connected to the auxiliary engines. The resulting electric power load is visualized in Fig. 6, for both time periods and both time resolutions. This adjusted system consisting only of four gensets and a total power load is hereby referred to as the “baseline system”. In the baseline system, the ME/SG is replaced by a main genset (MG).

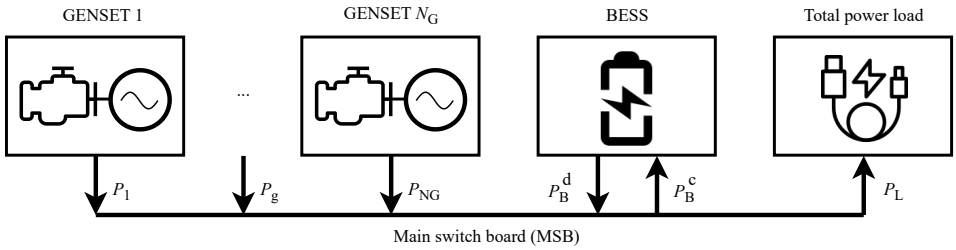

Figure 3: Illustration of the main switch board of the suggested vessel, with connected components and power balance.

2.2 Suggested System and Optimization Problem

The suggested system consists of N_G generator sets (gensets, G) each consisting of an engine and a generator, and a battery energy storage system (bess, B), which together serve the total power load (L), as illustrated by Fig. 3. Additionally, the option to curtail power production is included. The optimization does not include mechanic loads such as the propeller connection in the existing system. The conducted analysis is limited to conventional marine gas oil (MGO). However, the optimization problem is flexible for other fuels to be included.

The instantaneous power balance of the components connected to the switch board is visualized in Fig. 3. The sum of the power produced from all generators and the net delivered power from the battery, minus any curtailed production, must equal the sum of the total power consumption. All the power parameters are as per unit power $p \in [0,\ 1]$, which is defined as their power P divided by their installed power capacities P^{N}. The power balance per time instant is given by Eq. (3a), and the resulting total fuel consumption rate $\dot{m}$ is found from Eq. (3b).

$$P_{\mathrm{L}}[i_{\mathrm{t}}] = \sum_{g=1}^{N_{\mathrm{G}}} p_g[i_{\mathrm{t}}] \cdot P_g^{\mathrm{N}} + (p_{\mathrm{B}}^{\mathrm{d}}[i_{\mathrm{t}}] - p_{\mathrm{B}}^{\mathrm{c}}[i_{\mathrm{t}}]) \cdot P_{\mathrm{B}}^{\mathrm{N}} - p_{\mathrm{Cu}}[i_{\mathrm{t}}] \cdot P_{\mathrm{Cu}}^{\max} \quad (3a)$$

$$\dot{m}[i_{\mathrm{t}}] = \sum_{g=1}^{N_{\mathrm{G}}} \bar{m}_g[i_{\mathrm{t}}] \cdot p_g[i_{\mathrm{t}}] \cdot P_g^{\mathrm{N}} \quad (3b)$$

The overall optimization problem is defined as a mixed-integer linear program (MILP). The optimization is solved using a problem-based approach, using the Optimization Toolbox in MATLAB and the external solver "intlinprog" from Gurobi™ (v. 10.0.3). Parts of the method is similar to the scheduling stage implemented in Hennum (2021), but includes some other components as well as more details and model precision.

The optimization scheme is set up to minimize the total system cost. The overall cost function J is defined as Eq. (4a), as the sum of the cost of the battery (C_{B}) and each genset g (C_g), as well as other costs introduced by expansions of the optimization problem with variables and constraints. The option to curtail overproduction is included to reduce any potential challenges meeting the otherwise hard optimization constraints, and is penalized with a cost C_{Cu}.

$$\min_{\boldsymbol{y}} J \quad \text{subject to}$$

$$J = \sum_{g=1}^{N_{\mathrm{G}}} C_g + C_{\mathrm{B}} + C_{\mathrm{Cu}} \quad (4a)$$

$$\boldsymbol{y} = [\boldsymbol{y}_g^{\mathrm{T}},\ \boldsymbol{y}_{\mathrm{B}}^{\mathrm{T}},\ \boldsymbol{y}_{\mathrm{o}}^{\mathrm{T}}]^{\mathrm{T}} \quad (4b)$$

$$\boldsymbol{y}_g = [p_g,\ w_g,\ b_g,\ \Delta p_g,\ z_g^{\mathrm{I}},\ z_g^{\mathrm{R}},\ z_g^{\mathrm{Su}},\ z_g^{\mathrm{Sd}}]^{\mathrm{T}}, \quad \forall\ g \in \{1,\ \dots N_{\mathrm{G}}\} \quad (4c)$$

$$\boldsymbol{y}_{\mathrm{B}} = [p_{\mathrm{B}}^{\mathrm{d}},\ p_{\mathrm{B}}^{\mathrm{c}},\ z_{\mathrm{B}}^{\mathrm{c}},\ w_{\mathrm{B}},\ b_{\mathrm{B}},\ q_{\mathrm{SoC}},\ d,\ D_{\mathrm{t}}^{\mathrm{cy}}, D^{\mathrm{cy}},\ D^{\mathrm{sh}},\ D]^{\mathrm{T}} \quad (4d)$$

$$\boldsymbol{y}_{\mathrm{o}} = [p_{\mathrm{Cu}},\ p_{\mathrm{G}}]^{\mathrm{T}} \quad (4e)$$

The optimization problem has the decision variables specified in Eqs. (4b)–(4e), for the gensets, the battery system and otherwise. All decision variables are non-negative, and they are normalized such that their values are limited to the range 0–1. In order to limit the range of the cost function, J, is expressed in million Norwegian crowns (MNOK). These two range reductions were done for numerical stability and precision of the solver.

Each of the components and their respective decision variables and costs are described in the following sections, followed by the applied optimization constraints.

2.2.1 Genset Models

The system includes several gensets, where every genset g has its own power decision variable $p_g \in [0,\ 1]$ representing the loading of the genset relative to the installed capacity. The different equations describing the gensets are presented in this section, together with their decision variables and constraints.

Genset Running and Installment Signals

A binary optimization variable $z_g^{\mathrm{R}} \in \{0, 1\}$ is used as a running signal for each genset, indexed by time. Similarly, a second binary optimization variable $z_g^{\mathrm{I}} \in \{0, 1\}$ is used as an investment or installment signal. Eq. (5a) enforces that the running signal is 1 for every time step where the genset power is nonzero, and Eq. (5b) enforces that the installment signal is 1 if the genset power is nonzero at any point over the optimization period. z_g^{I} is calculated directly from p_g instead of from z_g^{R} in order to be able to include each of the two parameters independently of the other.

$$z_g^{\mathrm{R}}[i_{\mathrm{t}}] \geq p_g[i_{\mathrm{t}}] \tag{5a}$$

$$z_g^{\mathrm{I}} \geq \sum_{i_{\mathrm{t}}=1}^{N_{\mathrm{t}}} \left(\frac{p_g[i_{\mathrm{t}}]}{N_{\mathrm{t}}} \right) \tag{5b}$$

Limitations on Number of Gensets

For redundancy purposes, it is required that at least $N_{\mathrm{G}}^{\min}$ gensets were installed, as enforced by the constraint Eq. (6a). For practical reasons like space limitation, it is required that a maximum of $N_{\mathrm{G}}^{\max}$ gensets were installed, as enforced by the constraint Eq. (6b).

$$\sum_{g=1}^{N_{\mathrm{G}}} z_g^{\mathrm{I}} \geq N_{\mathrm{G}}^{\min} \tag{6a}$$

$$\sum_{g=1}^{N_{\mathrm{G}}} z_g^{\mathrm{I}} \leq N_{\mathrm{G}}^{\max} \tag{6b}$$

Minimum Genset Power Output

The high values of the PSFC curve increase the cost of running the gensets on low loading. However, gensets typically cannot operate below a certain threshold power, typically called the idle power. In order to model the idle power, a minimum power is enforced by adding the constraint Eq. (7a), where the power of a running genset is limited downward to p_g^{idle}. This constraints the running signal to only be one if the genset is producing sufficient power. The maximum curtailed power is, as Eq. (7b) indicates, set as the idle power of the largest available genset.

$$p_g[i_{\mathrm{t}}] \geq p_{\mathrm{G}}^{\mathrm{idle}} \cdot z_g^{\mathrm{R}}[i_{\mathrm{t}}] \tag{7a}$$

$$P_{\mathrm{Cu}}^{\max} = p_{\mathrm{G}}^{\mathrm{idle}} \cdot \max\left(P_g^{\mathrm{N}}\right) \tag{7b}$$

Genset Startup and Shutdown

Starting and stopping gensets are both fuel and maintenance demanding, and should be kept to a minimum. The startup and shutdown of gensets should, thus, be monitored, and frequent starting and stopping should be avoided. For this purpose, two binary optimization variable were included for each genset, z_g^{Su} as a startup signal and z_g^{Sd} as a shutdown signal. In order for these to get the correct value, the constraints in Eq. (8) were included for the startup, and the constraints in Eq. (9) for the shutdown.

$$z_g^{\mathrm{Su}}[i_{\mathrm{t}}] \geq z_g^{\mathrm{R}}[i_{\mathrm{t}}] - z_g^{\mathrm{R}}[i_{\mathrm{t}} - 1] \tag{8a}$$

$$z_g^{\mathrm{Su}}[i_{\mathrm{t}}] \leq z_g^{\mathrm{R}}[i_{\mathrm{t}}] \tag{8b}$$

$$z_g^{\mathrm{Su}}[i_{\mathrm{t}}] \leq 1 - z_g^{\mathrm{R}}[i_{\mathrm{t}} - 1] \tag{8c}$$

$$z_g^{\mathrm{Sd}}[i_{\mathrm{t}}] \geq z_g^{\mathrm{R}}[i_{\mathrm{t}} - 1] - z_g^{\mathrm{R}}[i_{\mathrm{t}}] \tag{9a}$$

$$z_g^{\mathrm{Sd}}[i_{\mathrm{t}}] \leq 1 - z_g^{\mathrm{R}}[i_{\mathrm{t}}] \tag{9b}$$

$$z_g^{\mathrm{Sd}}[i_{\mathrm{t}}] \leq z_g^{\mathrm{R}}[i_{\mathrm{t}} - 1] \tag{9c}$$

Eqs. (8a) and (9a) ensure that the startup and shutdown signals are 1 when the running signal switches from 0 to 1 and 1 to 0, respectively. Eqs. (8b)–(8c) and (9b)–(9c) ensure that the startup and shutdown signals are 0 when the running signal remains unchanged, respectively, regardless of which value it has. These four constraints have the additional function of ensuring that the startup signal is 0 if the running signal switches from 1 to 0, and that the shutdown signal is 0 if the running signal switches from 0 to 1.

Uniform Genset Power Distribution

In steady-state operation it is desired to have a uniform ramping and relative loading of each running genset, instead of running gensets on very different loading. In order to achieve this, a decision variable $p_{\mathrm{G}} \in [0,\ 1]$ representing the common loading is introduced. This is enforced through the constraints in Eq. (10).

$$p_{\mathrm{G}}[i_{\mathrm{t}}] - p_g[i_{\mathrm{t}}] \leq 1 - z_g^{\mathrm{R}}[i_{\mathrm{t}}] \tag{10a}$$

$$p_g[i_{\mathrm{t}}] - p_{\mathrm{G}}[i_{\mathrm{t}}] \leq 1 - z_g^{\mathrm{R}}[i_{\mathrm{t}}] \tag{10b}$$

Genset Ramp Rate

A decision variable $\Delta p_g \in [0,\ 1]$ is introduced to control the ramping of the gensets. It represents how much the genset power has changed from the last time step, and is defined as the nonlinear equation Eq. (11a), which is linearized to the two constraints Eqs. (11b) and (11c). It is assumed that all gensets have a power of zero prior to the optimization period. The ramping is through the constraint Eq. (11d) limited upwards to a maximum value of 1 per time step in all situations. The ramping is further limited upwards to a maximum ramp rate $\dot{p}_g^{\max}$ through the constraint Eq. (11e). The startup and shutdown signals are included here in order to avoid that the maximum ramp rate requirement inhibits the solver from starting or stopping gensets without violating the constraint.

$$\Delta p_g[i_\mathrm{t}] = |p_g[i_\mathrm{t}] - p_g[i_\mathrm{t}-1]| \tag{11a}$$
$$\Delta p_g[i_\mathrm{t}] \geq (p_g[i_\mathrm{t}] - p_g[i_\mathrm{t}-1]) \tag{11b}$$
$$\Delta p_g[i_\mathrm{t}] \geq (p_g[i_\mathrm{t}-1] - p_g[i_\mathrm{t}]) \tag{11c}$$
$$\Delta p_g[i_\mathrm{t}] \leq 1 \tag{11d}$$
$$\Delta p_g[i_\mathrm{t}] \leq \dot{p}_g^{\max} \cdot \Delta t + z_g^{\mathrm{Su}}[i_\mathrm{t}] + z_g^{\mathrm{Sd}}[i_\mathrm{t}] \tag{11e}$$

It should be noted that the ramping variable is not constrained to follow the ramping exactly, as from equation Eq. (11a). It is, however, constrained to be between the ramping and the maximum allowed ramping by constraining it downwards through Eqs. (11b) and (11c), and upwards through Eqs. (11d) and (11e). In situations where the ramping cost is negligible, this could cause the ramp rate variable to deviate from the actual value. Any ramp rate that is considered as a result is, for this reason, calculated directly from p_g in Eq. (11a), instead of using the output Δp_g.

Genset Usage and Fuel Consumption

The details of the fuel consumption lie within the fuel efficiency of each engine, the gravimetric fuel density and the energy efficiency of the connected genset.

The total fuel-to-mechanic power efficiency is modeled through BSFC curves, which give information on how fuel-efficient an engine operates at different mechanical loads. Similarly, the total fuel-to-electricity efficiency is modeled through PSFC curves, which give information on how fuel-efficient a genset operates at different electrical loads. Lastly, some generators were modeled alone through efficiency curves. These were expressed as functions of either the mechanic input power or the electric output power, depending on the purpose of the model.

The BSFC and PSFC curves are denoted $\bar{m}_m$ and $\bar{m}$, respectively, and are expressed as the fuel consumption for different per-unit output power values. These take into account all losses from the lower heating value (LHV) of the fuel to mechanic power or electric output power, respectively. The genset efficiency curves are denoted η_g, and are expressed as the total efficiency for different per-unit power values.

The PSFC curves are too non-linear to in a meaningful manner be linearized using a single line. To fit in the MILP problem it was, thus, instead linearized by treating it as a piece-wise affine (PWA) function, defined by a set of points with linear functions in-between. At any point in time, the power-fuel consumption relationship can be described by maximum 2 of these points with a straight line in-between them. The relationship between the genset power and the PSFC can, thus, be described by weighing together the two nearest points. The number of points and distance between them were chosen based on how nonlinear the model is.

The PSFC requirements were enforced using a special ordered set of type 2 (SOS2). This was done by introducing a set of binary variables $b_g \in \{0,\ 1\}$ to indicate which line segment is active, and a set of decimal weights $w_g \in [0,\ 1]$ to weigh together the two adjacent PWA points. Both parameters have two dimensions: one for each linearization point (j_g) and one for each time step (i_t) over the scheduling horizon.

The SOS2 requires that for any feasible solution maximum two (and subsequent) of the binary variables are non-zero at any point in time, together forming one line-segment. Eq. (12d) enforces that only one line segment is active at any point in time, Eq. (12c) enforces that the point has to lie on a straight line between the two points, and the contiguity constraint Eq. (12e) enforces that the two chosen points have to be subsequent.

The decimal weights are combined with the fuel model data (p_g^{PWA} and $\bar{m}_g^{\mathrm{PWA}}$) to return the exact genset power and fuel consumption for each time step. The power output from the genset is found from Eq. (12a), and its fuel consumption rate is found from Eq. (12b). The mass of the fuel is calculated instead of the volume, since parameters like energy content and carbon content are related directly to the fuel weight.

$$p_g[i_\mathrm{t}] = \sum_{j_g=1}^{N_g^{\mathrm{PWA}}} w_g[i_\mathrm{t}, j_g] \cdot p_g^{\mathrm{PWA}}[j_g] \tag{12a}$$
$$\dot{m}_g[i_\mathrm{t}] = P_g^{\mathrm{N}} \cdot \sum_{j_g=1}^{N_g^{\mathrm{PWA}}} w_g[i_\mathrm{t}, j_g] \cdot \bar{m}_g^{\mathrm{PWA}}[j_g] \cdot p_g^{\mathrm{PWA}}[j_g] \tag{12b}$$
$$\sum_{j_g=1}^{N_g^{\mathrm{PWA}}} w_g[i_\mathrm{t}, j_g] = 1 \tag{12c}$$

$$\sum_{j_g=1}^{N_g^{\mathrm{PWA}}-1} b_g[i_\mathrm{t}, j_g] = 1 \tag{12d}$$

$$w_g[i_\mathrm{t}, j_g] \leq b_g[i_\mathrm{t}, j_g] + b_g[i_\mathrm{t}, j_g - 1] \tag{12e}$$

Data sheets from engine manufacturers give limited information on the fuel consumption at part-load, and rarely cover low loads in detail. Considering that fuel efficiency is highly influenced by the loading of the engine, it was necessary to have models of the whole power range 0–1 Wpu. To get this, characteristics of different gensets were obtained from gathered measurements. The aforementioned measurements from Sintef Ocean was used, in addition to some measurements which were gathered from experimental work in a lab.

Genset AG: Auxiliary Engines and Generators The fishing vessel has several auxiliary engines which supply one generator each. For these sub-systems, there were available measurements for both the fuel consumption, the mechanic power and the electric power. The fuel consumption measurements and measured electrical power were used to make a PSFC model ($\bar{m}_{\mathrm{AG}}(p_{\mathrm{AG}})$) directly, for auxiliary engines with a generator.

Genset MG: Main Engine and Shaft Generator On the existing vessel, the main engine (ME) is connected mechanically both to the propeller and to the shaft genset. There is, thus, not a direct relationship between the fuel measurements and the measured electric genset power. However, the mechanic engine power was measured, and could be used to find the fuel-to-mechanic power-efficiency. Due to lack of measurements for the mechanic power of the shaft genset, the efficiency of this could not be found directly. Instead, it's part-load efficiency was assumed to be similar to the other gensets. Under this assumption, the engine efficiency and the genset efficiency could be combined to find an estimated PSFC-curve ($\bar{m}_{\mathrm{e}}^{\mathrm{MG}}(p_g^{\mathrm{MG}})$) for the main genset (MG). The two efficiency models were expressed as functions of the electric load in order to get the correct per-unit power values.

Genset LG: Hybrid Energy Laboratory Experimental work was conducted in the Hybrid Energy Laboratory at NTNU in Ålesund, to obtain fuel measurements and electric power production at part-load. This was done together with the main author of Æsøy et al. (2022), where the same measurements are presented. These were used to make a PSFC model ($\bar{m}_{\mathrm{LG}}(p_{\mathrm{LG}})$) directly from the fuel and power measurements.

The three genset models which were found from the gathered measurements are visualized in Fig. 4. They had three different sizes, and the models show some deviations between the different equipment. The onboard auxiliary engines with gensets showed the best fuel performance. For almost all loads, the main engine with genset was the most fuel-efficient. Hennum et al. (2023) showed that the small local maxima around 0.4 Wpu originated from a reduced genset efficiency at part-load. The PWA points are distributed over the range 0–1, with the first point at 0, the second point at p_g^{idle} and the last point at 1. The rest are non-uniformly distributed between p_g^{idle} and 1, where the distance between each point is dependent on the curvature in order to capture the variations.

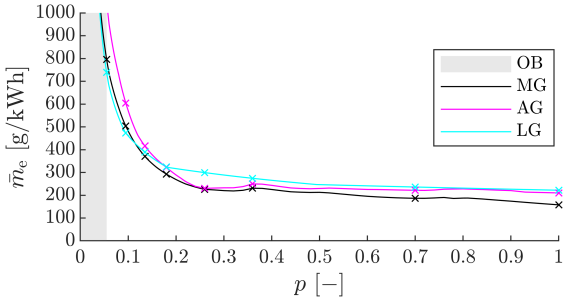

Figure 4: PSFC curves produced from gathered fuel and power measurements.

2.2.2 Genset Costs

There are costs related to installing and using the gensets, which are presented in this section. The genset cost C_g is calculated for each genset g from Eq. (13), as the sum of an investment cost C_g^{I}, a maintenance cost C_g^{M}, a fuel cost C_g^{F}, a startup cost C_g^{Su}, a shutdown cost C_g^{Sd} and a ramping cost C_g^{rr}. The five genset costs are dependent on if, how, how often, and how much each genset is installed and used.

$$C_g = C_g^{\mathrm{I}} + C_g^{\mathrm{M}} + C_g^{\mathrm{F}} + C_g^{\mathrm{Su}} + C_g^{\mathrm{Sd}} + C_g^{\mathrm{rr}} \tag{13}$$

Genset Investment Costs

An investment cost C_g^{I} was included for each genset, which gave a cost depending on whether or not the genset was used at any point over the scheduling horizon. The objective was to limit the number of gensets committed and used in the scheduling. To achieve this, the investment cost for each genset is defined by Eq. (14a), where c_g^{I} is the genset price, P_g^{N} is the installed power capacity of each genset and Δt is the time resolution of the optimization problem. It is not meaningful if the optimization solver weights investment costs for equipment meant to be used over many years with operating costs for a short time window. To avoid this without including many years of data

in one round of optimization, the investment cost was scaled in Eq. (14a) by the ratio between the optimization horizon and the expected genset lifetime T_g^{L}. To model the price drop for increasing size of the gensets, the price model in Eq. (14b) was used based on input from a company delivering gensets in a relevant size range. Here, P_g^{N} is given in W and the price is given in NOK/W.

$$C_g^{\mathrm{I}} = P_g^{\mathrm{N}} \cdot c_g^{\mathrm{I}} \cdot \frac{\Delta t}{T_g^{\mathrm{L}}} \cdot z_g^{\mathrm{I}} \cdot N_{\mathrm{t}} \tag{14a}$$

$$c_g^{\mathrm{I}} = 6.31 - 7.1 \cdot 10^{-8}\ P_g^{\mathrm{N}} \tag{14b}$$

Genset Maintenance Cost

A maintenance cost C_g^{M} was included for each genset, which was dependent on the number of running hours per genset. The objective was to limit the number of implemented gensets running simultaneously. This was calculated for each genset from Eq. (15), as the share of the genset installation cost calculated from the ratio between the running time and the expected genset lifetime T_g^{RL}. A relevant company gave an estimate that the accumulated maintenance cost is as large as the new-price after around 80 000 running hours.

$$C_g^{\mathrm{M}} = P_g^{\mathrm{N}} \cdot c_g^{\mathrm{I}} \cdot \frac{\Delta t}{T_g^{\mathrm{RL}}} \cdot \sum_{i_{\mathrm{t}}=1}^{N_{\mathrm{t}}} z_g^{\mathrm{R}}[i_{\mathrm{t}}] \tag{15}$$

Genset Fuel Costs

A fuel cost was included for each genset, to limit the amount of fuel consumed through optimal utilization of the overall energy system. The total fuel cost of each genset was found as the sum of its fuel consumption over all bins and time, multiplied with the fuel price. This is defined in Eq. (16), where the fuel density ρ_g^{F} and fuel-specific carbon density $k_g^{\mathrm{CO_2}}$ are included to get correct units. The PSFC value was not included as a separate optimization variable, in order to limit the size of the optimization problem.

$$C_g^{\mathrm{F}} = \left(\frac{c_g^{\mathrm{F}}}{\rho_g^{\mathrm{F}}} + c_{\mathrm{CO_2}} \cdot k_g^{\mathrm{CO_2}} \right) \cdot \Delta t \cdot \sum_{i_{\mathrm{t}}=1}^{N_{\mathrm{t}}} \dot{m}_g[i_{\mathrm{t}}] \tag{16}$$

Genset Ramping Costs

The ramp rate was penalized with the ramp rate cost C_g^{rr} calculated from Eq. (17a) with a ramping price c_{g}^{rr}.

$$C_g^{\mathrm{rr}} = \frac{c_g^{\mathrm{rr}}}{\Delta t} \cdot P_g^{\mathrm{N}} \cdot \sum_{i_{\mathrm{t}}=1}^{N_{\mathrm{t}}} \Delta p_g[i_{\mathrm{t}}] \tag{17a}$$

Genset Startup and Shutdown

In order to limit frequent starting and stopping, the startup and shutdown signals were penalized with the startup and shutdown costs C_g^{Su} and C_g^{Sd}, through the startup and shutdown prices c_g^{Su} and c_g^{Sd}, respectively. These were calculated from Eq. (18).

$$C_g^{\mathrm{Su}} = c_g^{\mathrm{Su}} \cdot P_g^{\mathrm{N}} \cdot \sum_{i_{\mathrm{t}}=1}^{N_{\mathrm{t}}} z_g^{\mathrm{Su}}[i_{\mathrm{t}}] \tag{18a}$$

$$C_g^{\mathrm{Sd}} = c_g^{\mathrm{Sd}} \cdot P_g^{\mathrm{N}} \cdot \sum_{i_{\mathrm{t}}=1}^{N_{\mathrm{t}}} z_g^{\mathrm{Sd}}[i_{\mathrm{t}}] \tag{18b}$$

The optimization itself assumes steady-state and does not take into account the time-, fuel- and maintenance cost-consuming transient startup and shutdown of the gensets. The startup and shutdown prices represent the transient startup and shutdown periods which are not addressed by the running signal.

The startup and shutdown prices are calculated from Eq. (19). The first part is the total fuel cost of running the genset on idle power (2nd PWA point) for a startup time Δt^{Su} and shutdown time Δt^{Sd}, respectively. The second part is the assumed investment cost related to the proportion of one startup/shutdown cycle assuming that the genset can take N_g^{S} startup/shutdown cycles before having to be renewed. Half of this last price is put on the startup, and half is put on the shutdown.

$$c_g^{\mathrm{Su}} = \frac{c_g^{\mathrm{F}}}{\rho_g^{\mathrm{F}}} \cdot \bar{m}_g^{\mathrm{PWA}}[2] \cdot p_g^{\mathrm{PWA}}[2] \cdot \Delta t^{\mathrm{Su}} + \frac{c_g^{\mathrm{I}}}{2 \cdot N_g^{\mathrm{S}}} \tag{19a}$$

$$c_g^{\mathrm{Sd}} = \frac{c_g^{\mathrm{F}}}{\rho_g^{\mathrm{F}}} \cdot \bar{m}_g^{\mathrm{PWA}}[2] \cdot p_g^{\mathrm{PWA}}[2] \cdot \Delta t^{\mathrm{Sd}} + \frac{c_g^{\mathrm{I}}}{2 \cdot N_g^{\mathrm{S}}} \tag{19b}$$

2.2.3 Curtail Produced Power

The option to curtail power was included by introducing a variable $p_{\mathrm{Cu}} \in [0,\ 1]$ in the power balance in order to address infeasibility issues that could arise from the periods with lower loads than the minimum genset power at the currently running genset. To include the curtailed power also makes it possible to handle fast down ramping of the load without getting infeasibility issues related to hard constraining of the maximum down-ramping of the gensets. The costs of curtailing power is calculated from Eq. (20), where c_{Cu} is the curtailing price. The absolute maximum allowed curtailed power is calculated as the idle power of the largest available genset.

$$C_{\mathrm{Cu}} = c_{\mathrm{Cu}} \cdot \Delta t \cdot P_{\mathrm{Cu}}^{\max} \cdot \sum_{i_{\mathrm{t}}=1}^{N_{\mathrm{t}}} p_{\mathrm{Cu}}[i_{\mathrm{t}}] \tag{20}$$

2.2.4 Battery Models and Costs

A battery pack is included with optional power and energy capacity. The battery is treated as a single battery regardless of its capacity.

The battery energy storage system is being discharged and charged throughout the operation of the vessel, where the positive power flow is defined out from the battery. The aforementioned $p_{\mathrm{B}}^{\mathrm{d}}$ and $p_{\mathrm{B}}^{\mathrm{c}}$ which enter the power balance in Eq. (3a) constitute the external power flow of the battery, as defined by Eq. (21a). The charging and discharging are, however, not ideal processes. To account for the resulting losses, discharging and charging efficiencies $\eta_{\mathrm{B}}^{\mathrm{d}}$ and $\eta_{\mathrm{B}}^{\mathrm{c}}$ are introduced, and the internal power $p_{\mathrm{B}}^{\mathrm{in}}$ which actually stores and releases energy can then be expressed as Eq. (21b). The nature of the efficiencies working opposite ways to either increase or decrease the internal power compared to the external power illustrates the need for splitting the battery power in its two components as a part of the linearization stage.

$$p_{\mathrm{B}}[i_{\mathrm{t}}] = p_{\mathrm{B}}^{\mathrm{d}}[i_{\mathrm{t}}] - p_{\mathrm{B}}^{\mathrm{c}}[i_{\mathrm{t}}] \tag{21a}$$

$$p_{\mathrm{B}}^{\mathrm{in}}[i_{\mathrm{t}}] = p_{\mathrm{B}}^{\mathrm{d}}[i_{\mathrm{t}}] \cdot \tfrac{1}{\eta_{\mathrm{B}}^{\mathrm{d}}} - p_{\mathrm{B}}^{\mathrm{c}}[i_{\mathrm{t}}] \cdot \eta_{\mathrm{B}}^{\mathrm{c}} \tag{21b}$$

The external battery power variables $p_{\mathrm{B}}^{\mathrm{d}}$ and $p_{\mathrm{B}}^{\mathrm{c}}$ are constrained to operate between 0 and the nominal power value $P_{\mathrm{B}}^{\mathrm{N}}$. To ensure that the battery is not charging and discharging at the same time, a binary optimization variable $z_{\mathrm{B}}^{\mathrm{c}}$ is introduced as a charging signal. The constraints related to the charging signal are given by Eqs. (22a) and (22b).

$$0 \leq p_{\mathrm{B}}^{\mathrm{c}}[i_{\mathrm{t}}] \leq z_{\mathrm{B}}^{\mathrm{c}}[i_{\mathrm{t}}] \quad , \quad z_{\mathrm{B}}^{\mathrm{c}} \in \{0,1\} \tag{22a}$$

$$0 \leq p_{\mathrm{B}}^{\mathrm{d}}[i_{\mathrm{t}}] \leq 1 - z_{\mathrm{B}}^{\mathrm{c}}[i_{\mathrm{t}}] \tag{22b}$$

The battery power is related to the battery state of charge (SoC) as described by Eq. (23a), which calculates how charged the battery is after time step i_{t}. The battery is to be used for peak-shaving and not as an energy source, and the final SoC is therefore set equal to an initial user-defined initial SoC, q_{SoC}^{0}, as enforced by the constraint in Eq. (23b). The nominal battery power is set from the installed energy capacity $E_{\mathrm{B}}^{\mathrm{N}}$ and a chosen maximum C-rate $\dot{n}_{\mathrm{B}}^{\max}$.

$$q_{\mathrm{SoC}}[i_{\mathrm{t}}] = q_{\mathrm{SoC}}^{0} - \frac{\Delta t \cdot P_{\mathrm{B}}^{\mathrm{N}}}{E_{\mathrm{B}}^{\mathrm{N}}} \sum_{i_{\mathrm{t}}=1}^{i_{\mathrm{t}}} p_{\mathrm{B}}^{\mathrm{in}}[i_{\mathrm{t}}] \tag{23a}$$

$$q_{\mathrm{SoC}}[N_{\mathrm{t}}] = q_{\mathrm{SoC}}^{0} \tag{23b}$$

$$P_{\mathrm{B}}^{\mathrm{N}} = E_{\mathrm{B}}^{\mathrm{N}} \cdot \dot{n}_{\mathrm{B}}^{\max} \tag{23c}$$

Similarly as for the generators, the battery is subject to costs related to both the investment/installation ($C_{\mathrm{B}}^{\mathrm{I}}$) and usage. For the battery, the latter is related to battery degradation ($C_{\mathrm{B}}^{\mathrm{D}}$) which speeds up the need for a reinvestment. The total battery cost is defined as the sum of these two costs, as given by Eq. (24).

$$C_{\mathrm{B}} = C_{\mathrm{B}}^{\mathrm{I}} + C_{\mathrm{B}}^{\mathrm{D}} \tag{24}$$

Battery Investment

The first battery cost is the investment cost $C_{\mathrm{B}}^{\mathrm{I}}$, which was included regardless of whether the battery is used or not. The battery was assumed installed independent of cost-effectiveness and the installation cost was calculated as Eq. (25), where $c_{\mathrm{B}}^{\mathrm{I}}$ is the battery price. To achieve this, this cost was included only in the post-optimization cost calculation, not in the cost function. Similarly as for the gensets, the investment cost is scaled by the ratio between the optimization horizon and the expected shelf lifetime $T_{\mathrm{B}}^{\mathrm{sh}}$.

$$C_{\mathrm{B}}^{\mathrm{I}} = c_{\mathrm{B}}^{\mathrm{I}} \cdot E_{\mathrm{B}}^{\mathrm{N}} \cdot \frac{\Delta t}{T_{\mathrm{B}}^{\mathrm{sh}}} \cdot N_{\mathrm{t}} \tag{25}$$

Battery Usage and Degradation

The charging/discharging cycling of battery has a considerable impact on its degradation. The more degraded the battery is, the less of its lifetime is left and the sooner the ship owner needs to re-invest in a replacement battery. A degradation-cycling-related reinvestment cost is for this reason included, in order to limit the battery degradation from wrong usage and over-usage. Both shelf degradation and cyclic degradation are included in the full degradation model. This is inspired by Wang et al. (2016), with some adjustments. This degradation model is selected because it takes into account that frequent deep cycling accelerates the degradation, without requiring a highly advanced model. This cost is calculated from the battery price, the energy capacity of the battery and the total fraction (D) of the degraded battery capacity over the scheduling horizon, see Eq. (26a). The battery degradation represents a reduction in battery life and is set as the maximum of the shelf degradation (D^{sh}) and the cycle degradation (D^{cy}), as stated by Eq. (26b). This is enforced by introducing the constraints of Eq. (26c) and Eq. (26d).

$$C_{\mathrm{B}}^{\mathrm{D}} = c_{\mathrm{B}}^{\mathrm{I}} \cdot E_{\mathrm{B}}^{\mathrm{N}} \cdot D \tag{26a}$$

$$D = \max\{D^{\mathrm{sh}}, D^{\mathrm{cy}}\} \tag{26b}$$

$$D \geq D^{\mathrm{sh}} \tag{26c}$$

$$D \geq D^{\mathrm{cy}} \tag{26d}$$

Shelf Degradation

The shelf degradation was implemented through the assumption that a battery would last a certain amount of time $T_{\mathrm{B}}^{\mathrm{sh}}$ before needing to be replaced even when unused. This degradation of the battery is calculated as the ratio between the optimization horizon and the expected shelf life, as showed by Eq. (27).

$$D^{\mathrm{sh}} = \frac{\Delta t \cdot N_{\mathrm{t}}}{T_{\mathrm{B}}^{\mathrm{sh}}} \tag{27}$$

Cyclic Degradation

The cyclic degradation was implemented through the continuous degradation model Eq. (28a) from Duggal and Venkatesh (2015), which gives the number of expected charging cycles N_c^{CO} if discharging to various states of charge. The inverse of Eq. (28a) gives the expected degradation for a regular full charging cycle between a full battery and this state of charge. The two curves are visualized in Fig. 5.

$$N_c^{\mathrm{CO}} = k_{\mathrm{B1}} \cdot (1 - q_{\mathrm{SoC}})^{-k_{\mathrm{B2}}} \tag{28a}$$
$$d^{\mathrm{CO}} = \tfrac{1}{k_{\mathrm{B1}}} \cdot (1 - q_{\mathrm{SoC}})^{k_{\mathrm{B2}}} \tag{28b}$$

A number of $N_{\mathrm{B}}^{\mathrm{PWA}}$ PWA points were distributed uniformly over the range between $q_{\mathrm{SoC}}^{\min}$ and $q_{\mathrm{SoC}}^{\max}$, since the battery's SoC is limited to this range. To correct for the average error which comes from the curvature of the continuous model, each point is corrected by the average deviation between the continuous curve and the linearized curve in the adjacent bins. This introduces an error in each point, but reduces the overall error of the model. Only four and five PWA points are included for the two levels of precision, in order to limit the model size. Both the continuous model and the two PWA linearizations are visualized in Fig. 5, from which it appears that none of the linearizations deviate significantly from the continuous model. This is confirmed by mean absolute percentage error (MAPE) of 1.8797 % and 1.0429 %, and coefficient of determination (R^2) of 0.9997 and 0.9999, respectively.

Equivalent SOS2 constraints as for the generator fuel curve presented in Eq. (12) were enforced to linearize the battery degradation model. These are presented in Eq. (29), where binary variables (b_{B}) and decimal weights (w_{B}) are introduced. The three constraints enforce that only one line segment of the curve is active at any point in time, and that the two points defining it are subsequent. As Eq. (29) shows, both parameters have two dimensions: one representing each linearization point (j_{B}) and one representing each time step over the scheduling horizon (i_{t}).

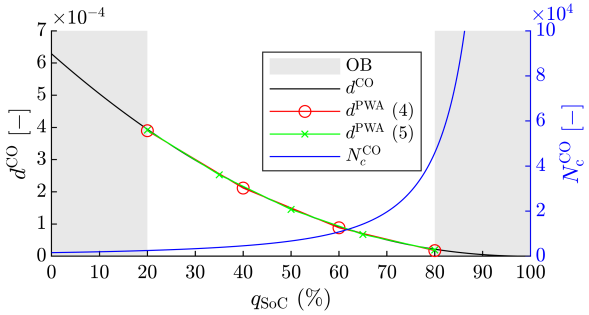

Figure 5: Battery degradation model including both the continuous (CO) model and the linearized PWA model, using 4 and 5 discretization points.

$$d[i_{\mathrm{t}}] = \sum_{j_{\mathrm{B}}=1}^{N_{\mathrm{B}}^{\mathrm{PWA}}} w_{\mathrm{B}}[i_{\mathrm{t}}, j_{\mathrm{B}}] \cdot d^{\mathrm{PWA}}[j_{\mathrm{B}}] \tag{29a}$$
$$q_{\mathrm{SoC}}[i_{\mathrm{t}}] = \sum_{j_{\mathrm{B}}=1}^{N_{\mathrm{B}}^{\mathrm{PWA}}} w_{\mathrm{B}}[i_{\mathrm{t}}, j_{\mathrm{B}}] \cdot q_{\mathrm{SoC}}^{\mathrm{PWA}}[j_{\mathrm{B}}] \tag{29b}$$
$$\sum_{j_{\mathrm{B}}=1}^{N_{\mathrm{B}}^{\mathrm{PWA}}} w_{\mathrm{B}}[i_{\mathrm{t}}, j_{\mathrm{B}}] = 1 \tag{29c}$$
$$\sum_{j_{\mathrm{B}}=1}^{N_{\mathrm{B}}^{\mathrm{PWA}}-1} b_{\mathrm{B}}[i_{\mathrm{t}}, j_{\mathrm{B}}] = 1 \tag{29d}$$
$$w_{\mathrm{B}}[i_{\mathrm{t}}, j_{\mathrm{B}}] \leq b_{\mathrm{B}}[i_{\mathrm{t}}, j_{\mathrm{B}}] + b_{\mathrm{B}}[i_{\mathrm{t}}, j_{\mathrm{B}} - 1] \tag{29e}$$

The cycle degradation $D_{\mathrm{t}}^{\mathrm{cy}}$ in each time instant is calculated as the difference between the degradation of two regular cycles, as stated by Eq. (30a). This nonlinear equation is enforced using the set of linearized constraints Eq. (30b) and Eq. (30c). The total cycle degradation is calculated as Eq. (30d).

$$D_{\mathrm{t}}^{\mathrm{cy}}[i_{\mathrm{t}}] = 0.5\,|d[i_{\mathrm{t}}] - d[i_{\mathrm{t}} - 1]| \tag{30a}$$
$$D_{\mathrm{t}}^{\mathrm{cy}}[i_{\mathrm{t}}] \geq 0.5\,(d[i_{\mathrm{t}}] - d[i_{\mathrm{t}} - 1]) \tag{30b}$$
$$D_{\mathrm{t}}^{\mathrm{cy}}[i_{\mathrm{t}}] \geq 0.5\,(d[i_{\mathrm{t}} - 1] - d[i_{\mathrm{t}}]) \tag{30c}$$
$$D^{\mathrm{cy}} = \sum_{i_{\mathrm{t}}=1}^{N_{\mathrm{t}}} D_{\mathrm{t}}^{\mathrm{cy}}[i_{\mathrm{t}}] \tag{30d}$$

2.3 Investigative Approach

The previously described optimization problem was implemented to achieve a flexible tool for isolated energy systems, such as a fishing vessel. The optimization tool was built by running several rounds of optimization using the existing gensets and power load, for battery sizes in the range 0–3 MWh in increments

Table 1: Parameters for the gensets and their models and fuel. The fuel parameters are given for 25 °C and 1 atm.

Parameter	Symbol	Value (MGO)	Unit	Source
No. PWA points in PSFC curve	N_g^{PWA}	9	–	–
Maximum No. startups	N_g^{S}	10 000	–	–
Maximum number of gensets	$N_{\text{G}}^{\max}$	4	–	–
Startup time	Δt^{Su}	15	min	–
Shutdown time	Δt^{Sd}	5	min	–
Idle power loading	p_g^{idle}	5.5	%	–
Ramping limitation	$\dot{p}_g^{\max}$	40	%/min	–
Ramping price	c_g^{rr}	1	NOK min/MW	–
Expected total life	T_g^{L}	25	yr	–
Expected economic running life	T_g^{RL}	80 000	h	–
Fuel density	ρ_g^{F}	0.855	$\text{kg}_{\text{fuel}}/\text{L}_{\text{fuel}}$	–
Fuel price	c_g^{F}	10	$\text{NOK}/\text{L}_{\text{fuel}}$	Bunker (2024)
Fuel energy density	e_g^{F}	42.7	MJ/kg	–
Fuel carbon intensity	$k_g^{\text{CO}_2}$	3.138	$\text{t}_{\text{CO}_2}/\text{t}_{\text{fuel}}$	–

of 100 kWh. An increasing number of constraints and costs were included in order to address unwanted usage of the system, as described in Sec. 2.3.1.

When completed, the tool is meant to be used for two purposes, first for sizing and system design, and secondly for scheduling and performance analysis. The choice between the two applications were controlled using the input parameters, the number of components included and the resolution of the input models and parameters. The choice of genset configuration from a first design stage was used further in a performance analysis. The scheduling stage is tested as described in Sec. 2.3.3, where a large range of genset sizes are made available for the optimization problem to choose from.

The second stage was then run for both the baseline system from Sec. 2.3.1 and the suggested system from Sec. 2.3.3, in order to evaluate the fuel saving potential by running the system in a more cost-efficient way. This is described in Sec. 2.3.4, where the results from these two systems are compared.

A set of default parameters was set, which is used everywhere in the presented research, where otherwise is not explicitly stated. The genset parameters are presented in Tab. 1, which includes parameters related to the genset and associated fuel. The battery parameters are included in Tab. 2, and remaining parameters are included in Tab. 3.

The maximum C-rate $\dot{n}_{\text{B}}^{\max}$ is set in order to give the system an available dispatchable power to handle faster variations in the load than is included in the optimization problem. The battery price is set based on a rough estimate of the total price for a battery system with inverter from Sustainable Ships (2024), where an inverter of 50 % higher capacity than the chosen maximum C-rate is used, again for the purpose of leaving a certain available power for the quicker variations.

The results were compared to the baseline system with the adjustment of replacing the mixed mechanic/electric ME+SG+Pr solution with the suggested MG+M+Pr solution, in order to avoid imprecision introduced by the assumptions linked to this change.

A series of tests were conducted in order to evaluate the functionality of the optimization problem and the results of applying it on data from an existing vessel. These tests are presented in Tab. 4, which shows which data selection (DS), genset selection (GS) and different constraints and parameter values were used in each test. Cells marked with "–" imply that the associated constraint and/or cost is not included in the optimization, whereas a price of 0 indicate that the associated variable is included in the optimization problem but not penalized in the cost function. Only decision variables which are constrained either through hard constraints or penalized in the cost function with a nonzero price are included in the optimization problem, in order to limit the problem size and solver time. Only nonzero costs are included in the cost function, in order to limit the model size and avoid potential numerical issues.

The three data selections are visualized in Fig. 6, where DS2 is a subperiod of DS3. In the selected periods, only the main engine was used. The results of the optimization was for this reason compared to the whole load P_{L} being delivered from the main engine. The system is, in other words, transformed into the same setup as the optimization is basing its analysis on, as visualized in Fig. 3.

GS1 is the four baseline gensets P_g^{N}, with the corresponding fuel curves presented in Fig. 4: One of size 4 MW (G1), two of size 650 kW (G2–3) and one of size 326 kW (G4). GS2 has in addition to GS1 a series of gensets available with installed power {350, 450, 550, 750, 850, 950, 1000, 1500, 2000, 2500, 3000, 3500} kW,

Table 2: Parameter data for the battery energy storage system.

Parameter	Symbol	Value	Unit	Source
Maximum battery charge/discharge C-rate	$\dot{n}_{\mathrm{B}}^{\max}$	1	h^{-1}	–
Battery price	$c_{\mathrm{B}}^{\mathrm{I}}$	5.5	MNOK/MWh	Sustainable Ships (2024)
Expected battery shelf life	$T_{\mathrm{B}}^{\mathrm{sh}}$	10	yr	–
Initial/final SoC	q_{SoC}^{0}	50	%	–
Minimum allowed SoC	$q_{\mathrm{SoC}}^{\min}$	20	%	–
Maximum allowed SoC	$q_{\mathrm{SoC}}^{\max}$	80	%	–
Degradation model coefficient	k_{B1}	1591.1	–	Wang et al. (2016)
Degradation model exponent	k_{B2}	2.089	–	Wang et al. (2016)
Battery discharging efficiency	$\eta_{\mathrm{B}}^{\mathrm{d}}$	91.0	%	Fortenbacher et al. (2017)
Battery charging efficiency	$\eta_{\mathrm{B}}^{\mathrm{c}}$	91.0	%	Fortenbacher et al. (2017)

Table 3: Other system parameters.

Parameter	Symbol	Value	Unit	Source
El-motor efficiency	η_{M}	90	%	–
Price for curtailing power	c_{Cu}	0	NOK	–
Currency exchange rate	–	11.5	NOK/EUR	–
Currency exchange rate	–	10.5	NOK/USD	–
Carbon price	$c_{\mathrm{CO_2}}$	0	NOK/$\mathrm{kg_{CO_2}}$	–

Table 4: Overview of the different parameters included in the different tests. The abbreviations stand for data selection (DS), genset selection (GS), include startup/shutdown cost (ISSC), include idle power (IIP), include curtailed power (ICP), include maximum ramp rate (IMRR) and enforce uniform power distribution (EUPD). Eq. refers to which constraint or cost it activates.

Expl./symbol:	DS	GS	Δt	N_g^{PWA}	$N_{\mathrm{G}}^{\min}$	ISSC	IIP	ICP	IMRR	EUPD
Unit:	[–]	[–]	[min]	[–]	[–]	[–]	[–]	[–]	[%/min]	[–]
Eq:					Eq. (6a)	Eq. (8), Eq. (18)	Eq. (7a)	Eq. (20)	Eq. (11e)	
Test 1A	1	1	1	5	–	–	–	–	–	–
Test 1B	1	1	1	5	2	–	–	–	–	–
Test 1C	1	1	1	5	–	Yes	–	–	–	–
Test 1D	1	1	1	5	–	–	Yes	–	–	–
Test 1E	1	1	1	5	–	–	–	Yes	–	–
Test 1F	1	1	1	5	–	–	–	–	Yes	–
Test 1G	1	1	1	5	–	–	–	–	–	Yes
Test 1H	1	1	1	5	2	Yes	–	–	–	–
Test 1I	1	1	1	5	2	Yes	Yes	–	–	–
Test 1J	1	1	1	5	2	Yes	Yes	Yes	–	–
Test 1K	1	1	1	5	2	Yes	Yes	Yes	Yes	–
Test 1L	1	1	1	5	2	Yes	Yes	Yes	Yes	Yes
Test 2A	2	2	5	4	4	Yes	Yes	Yes	Yes	Yes
Test 2B	2	2	1	5	4	Yes	Yes	Yes	Yes	Yes
Test 3A	3	1	5	4	4	Yes	Yes	Yes	Yes	Yes
Test 3B	3	1	1	5	4	Yes	Yes	Yes	Yes	Yes
Test 3C	3	2	5	4	4	Yes	Yes	Yes	Yes	Yes
Test 3D	3	3	1	5	4	Yes	Yes	Yes	Yes	Yes

which gives the solver flexibility to choose a suitable selection of genset sizes. GS3 is a result of choices based on test 3A, where the selection is reduced by removing gensets which are not chosen for any battery size. Each genset has their own PSFC curve, which for the additional gensets were set as the AG model. An overview of the included gensets is included in Tab. 5.

In the two years of existing data, the ramp rate exceeded 20 %/min less than 0.05 % of the time for the generators and less than 0.25 % of the time for the main engine. The ramp rate was somewhat higher for larger gensets than the smaller. However, in the time period in question with chosen time resolution, the maximum ramp rate of the total load was over 37 % of the nominal power of the main engine per minute when Δt was 1 min and 6.7 %/min when Δt was 5 min. An absolute maximum ramp rate of 40 %/min was for this reason expected to not be too restrictive, although it arguably is a bit high if occurring often and at low loads. Maximum ramp rates of 15 and 20 %/min were tested, but increased the solver time drastically and seemed unreasonably strict considering the variations in the data.

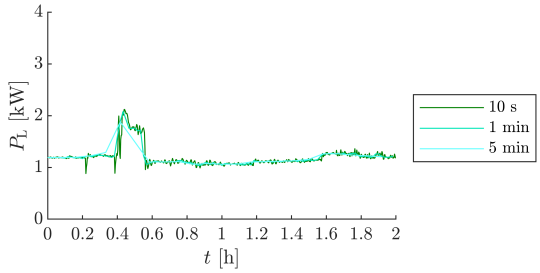

(a) Period DS1.

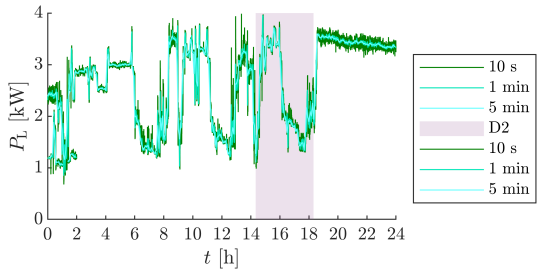

(b) Periods DS2 and DS3

Figure 6: Total electric power load for the three data selections, with three time resolutions.

Table 5: Available gensets and their corresponding PSFC model in each genset selection.

P_g^N [kW]	GS	PSFC
4 000	1, 2	MG
3 500	2	MG
3 000	2	MG
2 500	2, 3	MG
2 000	2	MG
1 500	2, 3	MG
1 000	2	MG
950	2	AG
850	2	AG
750	2	AG
650	1, 2	AG
650	1, 2	AG
550	2	AG
450	2	AG
350	2, 3	AG
326	1, 2, 3	LG

The ramping price is tuned in order to try to make the battery take a large share of the fast load variations without ending up curtailing power.

2.3.1 Evaluation and Expansion of Optimization Problem

The optimization was at first run several times in tests 1a–h, gradually increasing the complexity of the optimization problem. This was done in order to evaluate and address potential weaknesses by adding different constraints to remove unwanted behaviour. At first, a minimum genset requirement was included to address redundancy requirements for scenarios when the genset otherwise would choose to only install one genset. A startup price was then added in order to limit the number of times the installed gensets would start and stop with associated frequent ramping. A minimum genset power was included to represent the idle power, and at the same time the option to curtail power was included to avoid infeasibility issues. The reasoning for setting the price for curtailed power to 0 is that it already is penalized indirectly through the fuel consumption.

A data selection covering 2 hours of operation was used for the evaluation of the optimization problem. In order to evaluate the tool effectively, a period where the main engine was run inefficiently on low load was chosen. This way, it was certain that the fuel consumption and genset configuration would be chosen differently if the optimization did its job.

2.3.2 Validation of Model Size Reduction

One large challenge with the optimization approach using such detailed models is the solver time. To address this, tests 2a–b were run in order to evaluate if the results would vary largely if the time resolution was decreased by increasing Δt from 1 to 5 minutes, and the battery degradation model was made slightly less precise, using 4 instead of 5 discretization points. This was done with the full optimization problem from test 1h, but with a longer load series which covered a more representative range of the current usage of the vessel.

2.3.3 Optimize Genset Configuration

The outputs from the optimization problem are in Secs. 2.3.1 and 2.3.2 evaluated on an aggregated basis per test for each optimization problem, to evaluate the overall performance of the optimization problem given different constraints and parameters. The next step is to use the optimization problem in the two aforementioned steps to first find an optimal genset configuration and second an optimal battery size. Tests 3A and 3B were run in order to get results for the existing genset configuration. Test 3C was then run to find an optimal genset configuration, using a low resolution of the time series and battery degradation model.

A minimum/maximum number of installed gensets were set to 4, to force the solver to suggest a similar genset configuration as the existing system with more optimal installed power capacities, for comparison purposes. Here, the investment costs were included for the gensets, to limit the installed capacity.

The configuration was then used in test 3D, where the resolution was increased in order to get more detailed results. The final performance of the system

operation in 3D was then evaluated to consider future adjustments.

For the genset configuration, battery sizing and performance analysis, a data selection covering 24 hours of operation was used. The measurements covered a period with power-demanding operations, where the main engine was loaded more heavily. This data selection contained power variations within a range representative of the rest of the gathered measurements. The data selection includes periods with both transit, searching and trawling activities south-west of Lofoten, Norway. The investigated journey started and ended with the vessel far away from the coast, and it stayed at sea the whole time.

2.3.4 Battery Sizing and Performance Analysis

A performance analysis was run to investigate the potential fuel and cost savings compared to the current usage of the baseline system. This was done for both the baseline and alternative suggested genset configurations, for a range of battery sizes. The same calculations were done on the measurements from the existing system as for the optimized usage, as a benchmark. In this design stage, higher resolution models and data were used as a trade-off between result accuracy and computational effort.

To investigate the potential that lies within utilizing the existing system more optimally, test 1j from 2.3.1 was run again. This time the minimum number of gensets $N_{\mathrm{G}}^{\mathrm{min}}$ was set to 4, to force the installation of all gensets regardless of what is cost-optimal given the limited number of data points in the input load.

To investigate the potential that lies within more optimal sizing of the equipment and still utilizing the system optimal given the previously presented constraints, the analysis in Sec. 2.3.3 was run again, now again with minimum 4 gensets installed.

3 Results and Discussions

The results from running the presented optimization problem using data from a fishing vessel in operation are presented in this section. At first, the behaviour of the optimization problem, including different constraints and costs, is presented in Sec. 3.1. A validation of the results using two different models and data resolutions are presented in Sec. 3.2 before the two-step design and analysis process using the two resolutions is presented in Sec. 3.3. The performance is addressed in Sec. 3.4 before discussing different aspects of the results further in Sec. 3.5.

3.1 Evaluation and Expansion of Optimization Problem

The model was tested and expanded as needed, to address a series of unwanted behaviour, and the described behaviour is considered somewhat more interesting than the values themselves in this part. This section describes how the different constraints changed the results. It should be noted that the optimization framework is currently not yet tested on a large variety of data with a large library of different gensets available, and that the behaviour described here may vary somewhat with different load profiles.

It was observed that the solver installed as few and as small gensets as possible, which in some cases for test 1A was only one. This happened both in cases where only a few genset sizes were included and the battery was small, and in cases where there were included many genset sizes (flexible capacity choice) and the battery capacity was large enough to let the battery serve the peaks in the power demand.

With a low or no ramping limit, ramping cost or startup cost, the solver chose in some situations to increase the number of startups and shutdowns to 6 times per hour. This happened mainly for large battery capacities where the battery could be used instead of one of the gensets for longer periods, but it did at the same time increase the solver time 800-fold when the ramping limit was included. When introducing a ramping price which was high compared to the curtailing price, the algorithm chose to run the gensets on a very steady, higher than necessary loading instead of frequent rapid ramping, while letting the variations be covered by curtailment instead of adjusting the genset loading. This was the situation when the battery size was not large enough to cover these load variations by itself.

Additional adjustments could be to change how the maximum allowed curtailed power is calculated, or in other ways limit the curtailed instantaneous power or accumulated energy further. Another adjustment could be to relax the ramping limit and reduce the ramping price. Further effort could be put into estimating a reasonable ramping price based on the fuel price, which is just small enough to avoid curtailing power instead of ramping the gensets.

The ramping price was then reduced to the low value found in Tab. 4 to address the overly steady genset power and power curtailment. Including the constraints Eqs. (18a) and (18b) reduced the number of startups to maximum 1–2 and the number of shutdowns to 0–1. At the same time the fuel reduction became zero or negative for cases with small to no battery capacity, and stayed around 9 % compared to the current system, for medium to large batteries ($\geq$ 800 kWh) using DS-1. It further had a limiting ef-

fect on the desired number of installed gensets by 1–2 units, installing larger gensets with a lower number of running hours. Otherwise the results were not largely impacted by an increased startup price, but the solver time got reduced significantly.

One of the main challenges is the optimization time, which could increase significantly for some combinations of constraints and constraint parameters. In particular, this was a challenge with the hard ramp rate constraint Eq. (11d), which when lowered below the maximum ramping of the input data compared to the MG was increased by a 400-fold.

The optimization chose to install and use only the main genset and the emergency genset for battery sizes below 800 kWh, whereas only the two auxiliary gensets were chosen for larger battery sizes. The fuel savings were purely from the battery enabling running smaller higher loaded gensets, which was apparent from the fuel savings not being further impacted past this point.

The introduction of a maximum ramp rate through constraint Eq. (11e), reversed the unwanted usage which in some cases lead to a large fuel increase. After the startup and shutdown signals were included, this constraint did not limit the number of starting and stopping of gensets. It increased in some situations the optimization time by an unreasonable amount when included alone, but the increase was not notable when included together with the aforementioned other constraints and costs.

The battery usage and degradation was increased as the genset usage was limited more and more when the battery was lower than 500 kWh. At this point, the battery size got large enough for the cycling degradation to become smaller than the shelf degradation. This was the case up until the battery size got large enough to cover the full load peak and reduce the genset size. At this point, the total degradation increased to 280 % of the shelf degradation. From this point, the battery size increased without changing its use remarkably, and the relative degradation did, for this reason, get lower from this point. For battery sizes above 2 200 MWh, the cyclic degradation again became smaller than the shelf degradation.

Summary of the final behaviour

For small batteries, the solver chose to only run a single large genset. When the battery size increased, this enabled using the two AG's. The solver time of the final optimization model was relatively short, and managed to not curtail power in the test scenarios 1A–L. The fuel consumption increased slightly when the battery capacity was small, but was instantaneously reduced by 9.2 % when the battery size enabled only using smaller gensets. The number of startups and shutdowns were kept to a maximum of 2 and 0, respectively.

Larger battery sizes enable fewer and smaller gensets to be installed, with a lower total installed capacity. The total number of startups and shutdowns were higher for larger battery sizes, due to the battery increasingly being used in the power-balancing of the system, and as temporary energy-storage during operation. The number of running hours was increased due to several small gensets being run simultaneously instead of fewer large gensets.

A power controller based on such an optimization problem can end up increasing fuel consumption in order to limit other costs. It is important to make sure the optimization problem is properly tuned based on the relevant load profile and variations. The aforementioned investment in smaller gensets to limit the investment and maintenance costs, and curtailment of power in order to avoid ramping are two examples of this.

The solver avoids starting a genset before strictly necessary, in order to save fuel and maintenance costs. On the other hand, it avoids shutting down a genset it started when the load increased, even when returning to the same loading where it at first only ran one, since it considers it more expensive with frequent starting and stopping than running on a slightly lower fuel-efficient loading for a period.

The maximum genset ramp rate is only 20 %/min under operation, and this occurs less than 0.07 % of the time. The ramp rate is below 10 %/min 99.2 % of the time and below 5 %/min 98.4 % of the time. This despite the maximum possible ramp rate being set to 40 %/min. More rapid ramping only occurs when starting and stopping the gensets, and it is assumed that the battery would take the even more rapid power variations by increasing the maximum C-rate. The ramping limitation seems, for this reason, to be strict enough as it is.

The ramp rate constraint should be softened by introducing a penalized slack variable. When setting a low ramping price, the battery is almost not used. But when including one of 10 NOK/MW, the genset ramping is more limited and the battery is increasingly used. It is hard to find a value for the ramping price which is objectively better than others, although it is an option to tune it until the results become somewhat reasonable. Some further effort should be out into investigating reasonable ramping prices.

The idle power constraint is softened through the opportunity to curtail power, although there is a maximum possible curtailment of $P_c^{\max}$ available. The results suggest that this approach works as intended by ensuring feasible solution when the power balance requirements, ramping limitations or other hard constraints become too strict.

3.2 Validation of Model Reduction and Genset Configuration

The test of using two different time resolutions gave similar but not equal results. The differences are presented in the following section.

The solver time increased significantly when using a time resolution of 1-minute data instead of 5, particularly for small battery sizes. At the most, the solver time was increased 280-fold. This was for a scenario where the option to use the battery existed, but the available battery power was low. This is more important for the method's feasibility than it says something about the results themselves.

The main difference between using the two different time resolutions is apparent from tests with a battery size relatively small compared to the next step down in genset size. When the time resolution is lowered, the power peaks are somewhat smoothed, which reduces fast variations and the highest peaks in the load. This was observed to enable the solver to reduce the size of both the installed gensets and the currently running gensets and, by doing this, increase the fuel efficiency for systems with smaller batteries in the low-resolution situation than in the high-resolution situation. The overall trend was, however, the same. Furthermore, the genset configuration, fuel savings and battery degradation ended up the same when the battery size got large enough.

The installed power capacity of the four gensets was reduced when the battery size was increased, and this happened for smaller batteries when the time resolution was low. This is arguably because the averaging of the data input dampens the load variations, which in turn puts lower strain on the genset ramping and need for available power from the battery. It is, thus, possible to install smaller gensets for slightly smaller battery sizes when the time resolution is lowered.

It should be noted that the power varies considerably more than its minute mean values. As Fig. 6 shows, the total 10 s average power has some larger variation and the original 1 s values have even more fluctuations, but the difference is not extreme relative to the total load. These variations could, however, be quite large compared to the installed power of the battery unit and should, thus, be taken into account when deciding on the SoC limits in this initial design stage to get results which can be considered representative. This shows that a necessarily big power buffer should be given to the battery, so it is able to take the even shorter variations. It could be a good idea to keep the C-rate as it is in this scheduling stage, instead of letting it utilize higher power values since the highest time resolution here is 1 minute and the measured data is on second basis.

The lowering of the maximum allowed C-rate for the five-minute resolution by 1/5 was seemingly a bit strict, considering that moving over to minute data enabled installing smaller gensets for the same battery sizes, despite the power variations being larger. One alternative route could be to find a better scaling value from the actual frequent minute variations around the five minute mean.

It should be noted that the step in installed genset capacity is large, with a maximum of 500 kW, which arguably gives a somewhat un-nuanced result. However, it is worth noting that all the current gensets are included and the optimization still finds it the most cost-efficient to only run the MG when no or only a small battery is installed. This supports the current usage of the vessel in the period. The result is that the remaining installed 3 gensets are the smallest ones instead of what would fit the best in certain time periods if other types of the vessel's operations had been included in the time series.

One notable finding is that the fuel savings are sacrificed to buy smaller and thus cheaper gensets when the battery size is increased. The solver chooses to invest in a smaller total genset capacity and instead let the fuel consumption increase, when the battery becomes large enough to deal with sufficiently large power variations. This gives an increase of 10 % in fuel consumption instead of a reduction. This is a weakness with having all gensets available for the optimization solver to choose to install or not, but illustrates an important point when designing the system: The overall cheapest system is not necessarily the most fuel-efficient system, since the capital cost and other operating costs in some situations can outweigh the advantage of minimizing the fuel consumption.

In the range of battery sizes where the peak-shaving effect is still too small to enable a large reduction in installed capacity, the existing main engine and emergency genset are chosen by the solver. Additionally, the other two smallest defined gensets were installed. This is because the solver chooses to only run on the main engine, like the current usage and chooses to buy the smallest and, thus, cheapest gensets to fill up the requirement of using four gensets. This is another weakness of the current analysis, since the results are based on such a short time series. This might not happen in other periods of the total time series. A natural next step is to use a longer timeseries which is overall more representative for the range in the operation of the vessel.

The interesting part of implementing the two PWA models together is that using the battery to peak-shave the genset power can lead to more fuel-efficient operations which saves cost. On the other hand, the

power-losses and increased battery degradation from-frequent and deep charging/discharging charging cycles is also costly. Furthermore, this leads to a cost-balance needed to be found between fuel-efficient genset usage and battery usage.

The resulting genset selection and fuel reductions are presented in Figs. 7 and 8. The five minute evaluations are capable of suggesting the same genset installed power capacity and approximately the same configuration as the one minute evaluation. The fuel consumption is not completely the same when the battery becomes large enough, but this is not an issue considering that it is the genset configuration which is the desired outcome of the first stage.

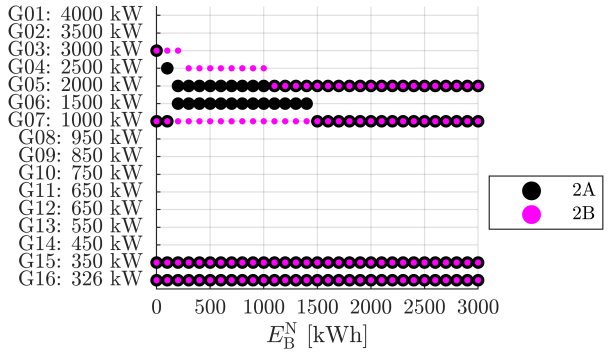

Figure 7: Installed gensets, for systems with different battery sizes.

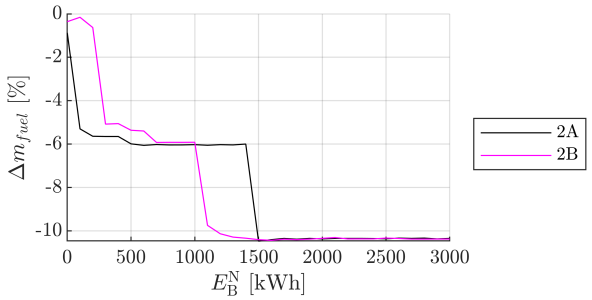

Figure 8: Change in fuel consumption compared to current system, for systems with different battery sizes.

The gensets and batteries must operate together to cover both the load and the rapid variation in load. A battery can both cover fast variations in the power load and larger variations which enable running on smaller gensets than the maximum load. However, installing a large battery to cover the maximum power peaks leads to a bad degree of utilization of the battery system. This is costly compared to the saved stress of the gensets and reduced fuel consumption. The choice of battery size must take this into account. For the current vessel, a battery power of 650 kW will cover 99.25 % and 98 % of the power variations around the one and five minute mean values, respectively.

By excluding 1 % of the time, the total power load has second-based power variations above the one and five minute mean data of 580 og 900 kW, respectively. With a C-rate of 2.5, this requires battery sizes of 232-360 kWh.

Frequent starting and stopping engines/gensets does not occur in the existing settings and load data. There were some situations, however, where one single genset was started for only one time step, a period of five minutes. Since frequent starting and stopping was not a problem for the investigated load series, it is not addressed through additional constraints. A natural next step could, however, be to implement minimum uptime when being started and a minimum down-time when stopped, if frequent starting/stopping in some situations would become a problem.

3.3 Applying the Tool – System Configuration

The optimization was run in two stages, as described in Sec. 2.3. The first stage made a selection of gensets for each battery size, and a group of these were chosen. From running the optimization with only the chosen gensets, the second optimization was used to find a suitable battery size which gave the maximum fuel reduction.

Fig. 9 gives an overview of which gensets are installed for different battery sizes for tests 3A, 3B, 3C and 3D, which are only different in terms of time/model resolution and available gensets. The solver chooses to install two large gensets together with the two smallest gensets, instead of the current largest genset. One of the large gensets are preferably larger when the battery is excluded, as the figures show for test 3C which has all the gensets available. This also happened for some situations where the battery was installed but had a small capacity.

Fig. 10 illustrates the fuel savings compared to the current system, and shows that the system is able to save fuel in both test 3C and 3D. Test 3C and 3D show that a fuel reduction of around 0.9 % and 3.2 % can be achieved even with no battery, simply from better scaling and utilization of running gensets. The figure further shows how the fuel savings are increased with increased storage capacity of the battery system, and that around 6–7 % fuel reduction can be achieved. The solver chose here to at first only start one genset at a high loading, and then start another one when the power load increases, which is the main contributing factor to the fuel savings.

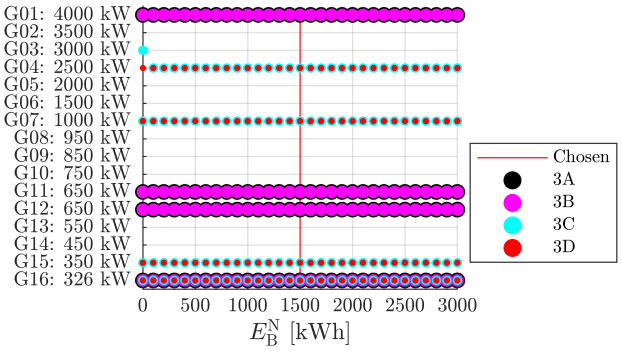

Figure 9: Installed gensets, for systems with different battery sizes.

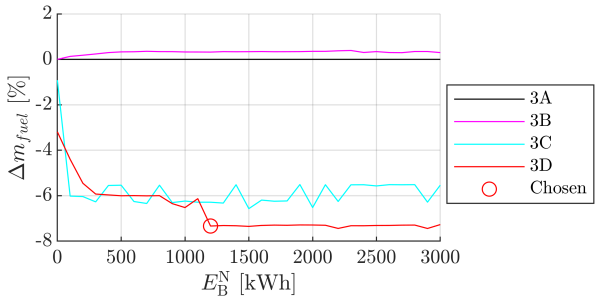

Figure 10: Relative change in fuel consumption compared to current system, for systems with different battery sizes.

Fig. 9 and 10 also show the results of tests 3A and 3B, which are using the current genset configuration. Here, the solver chooses to run almost without using the battery at all when the time resolution is low. When the time resolution is increased, the fuel consumption is increased by around 0.34 % when a battery is included. The time series of the power distribution reveal that this increase is due to the battery being used to limit the ramping of the gensets, and in this way giving a power loss which is larger than the power saved from increased genset efficiency. Here it should be re-iterated that the cost function is defined to minimize the total system cost, not to minimize the fuel consumption or emissions alone. This suggests that if the PMS is programmed with ramping of the gensets in mind without considering the fuel consumption, the overall fuel consumption could end up being increased through charging losses of using the battery. However, the currently presented increase of 0.34 % is small compared to the fuel savings in other presented results of 6–7 %.

The battery SoC is visualized for different battery sizes of test 3D in Fig. 11, and shows how the battery capacity is being utilized for a selection of sizes around where fuel savings change. The power distribution time series show that when the battery size is low, all four gensets are being used at some point with a number of genset startups as high as 7 times per 24 hours. This is arguably a high number considering that it is 24 hours of continuous operation of the fishing vessel.

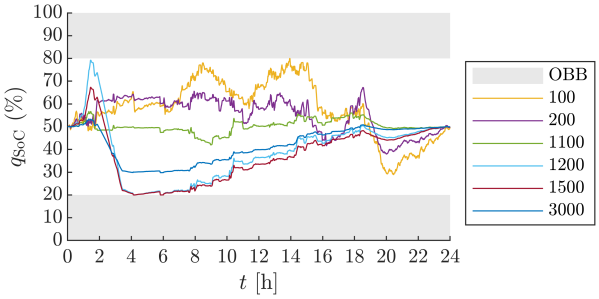

Figure 11: Battery SoC for test 3C, for a selection of battery sizes (kWh).

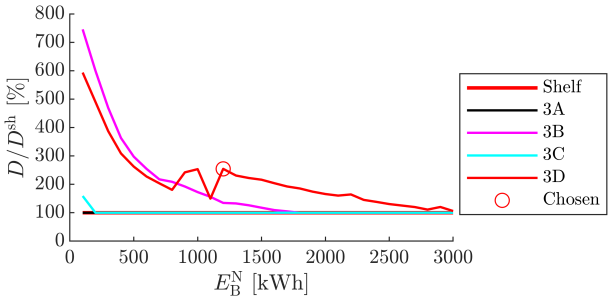

Figure 12: Battery degradation relative to the shelf degradation, for systems with different battery sizes.

Fig. 11 shows that when the battery capacity is as low as 100 kWh, the battery only contributes when some of the largest peaks in the power demand occur. This occurs around hours 8–12 and 15–16, and here the number of running hours is at 212 % compared to the optimization horizon and the fuel reduction is limited. When the battery size is increased to 200 kWh, the number of startups is reduced to 5, the fuel reduction is increased, the number of running hours is reduced and the battery lifetime is increased through reduced battery relative degradation. However, for such small battery sizes, the battery is mainly used to limit rapid ramping of gensets and not so much for peak-shaving.

Fig. 11 further shows that the battery capacity is not fully utilized for semi-large batteries before the capacity reaches 1 200 kWh, at which point the capacity is large enough to cover larger peaks in the demand. What happens from this point is further presented in the analysis section below.

The genset configurations for test 3C visualized in Fig. 9 are remarkably similar regardless of battery ca-

pacity when the time series of 24 hours is used. It was the same for almost all systems with sufficiently large batteries, with only some exceptions. When only 12 hours of data was included, this varied somewhat more for battery capacities between 1 400 and 1 700 kWh. This is in the lower range of where the battery capacity is large enough to cover more of the slower variations. This points to the length of the time series being important for getting unambiguous results. It is worth noting that the two most common combinations of large gensets all had the same total capacity of 3 500 kW, and that there is only one exception from the total genset power being of this dimension for battery sizes from 300 kWh.

When increasing the time resolution, the power variations for some situations increased enough for the chosen gensets to not give feasible solutions, given the otherwise unchanged input. This happened when the C-rate was kept unchanged regardless of time resolution and the battery was small enough to already be used to the maximum of its capacity. This was to a large extent solved by scaling the maximum C-rate with the time resolution as previously described, to open for the larger power variations in the one minute data than in five minute data. The current way of choosing different C-rates is not particularly exact, and a more precise way of deciding a time resolution-dependent maximum C-rate should be investigated further.

The genset configuration which most often occurs for all battery sizes is assumed to be a good choice and was used in test 3D. This increased the fuel reduction to 3.2 % when the battery was not included, rapidly increasing to around 6 % for battery sizes from 300 kWh. The percentage-wise reduction of CO_2 is the same as the fuel reduction since the same fuel is used in all cases.

As illustrated in Fig. 10, the fuel savings are increased further to around 7.3 % when the battery is increased past 1 200 kWh, at which point the battery is large enough to make the genset run more fuel-efficient. The cost reduction from increased fuel-efficient utilization of the gensets must at this point be large enough to compensate for the reduced system efficiency from temporarily storing the energy in the battery. The main reason for the fuel consumption to be reduced somewhat around 1 100 kW is that the battery at this point becomes large enough for the emergency generator of 326 kW not to be started.

It is worth noting that the battery can play two roles. One as a power buffer to cover short term fluctuations in the load, which requires a high C-rate but not necessarily a high energy capacity. The other one is as an energy storage, to cover slower-varying longer lasting power variations which require more energy if the C-rate also is high. When the time resolution is high, the battery power utilization of the battery was high, but not the changes in SoC. The battery has, in other words, more energy to give than what is being utilized in such a situation.

Choosing a battery capacity just above breakpoints like the one found in Fig. 10 which saves a lot of fuel when the battery is new is un-advisable. The battery capacity degrades over time and should be large enough over the whole lifetime. Considering that the SoC limitations are somewhat narrow at 20 % and 80 %, one solution could be to let this be increased to for example 20–90 % under operation in order to have more energy available. Another approach could be to make the battery a bit larger when new, to compensate for the capacity reduction over time, e.g. to take into account a 20 % drop in storage capacity over the lifetime which increases the necessary battery capacity from 1 200 to 1 500 kWh.

The accumulated battery degradation by the end of the optimization period is presented in Fig. 12. The degradation is presented relative to the shelf degradation, in order to express how much more the battery is degraded compared to not being used at all. This is due to the degradation saying something about how fast the ship owner needs to reinvest in a replacement battery. Fig. 12 shows that the relative battery degradation decreases with increasing battery size, except for when the increased battery size enables different and increased battery usage. Comparison of Figs. 10 and 12 clearly shows a trend where increased fuel savings occur when the battery is also used and, thus, degraded more.

Considering that the resulting selections for the most part are equal regardless of battery size, , the main difference going from test 3C to 3D is the time resolution, where the increased resolution introduces larger power variations which are covered by the battery. This explains the increased degradation for test 3D apparent in Fig. 12. It is worth noting that the battery degradation is the highest in tests where the fuel reduction is the highest.

The option of power curtailment was, as previously mentioned, included in order to address potential idle power-issues and ramping limitation issues. This also occurred when testing the model with different system parameters, and increased the fuel consumption noticeably. However, no energy was curtailed in any of the tests when using the final system parameters.

3.4 Analysis of Chosen System

The final chosen system configuration consisted of the gensets $P_g^{\mathrm{N}} \in \{2\,500,\ 1\,000,\ 350,\ 326\}$ kW and a battery of size 1 500 kWh. These are indicated in Figs. 9

and 10, and the next paragraphs present the most interesting detailed output from the optimization problem for this exact system. This is solely based on the aforementioned parameters, and any challenges related to weight or volume are not considered here.

The power distribution over time is visualized in Fig. 13, which shows that only one genset is started at first, with the remaining power being delivered by the battery. The main difference between the results using this 1 500 kWh battery with a fuel saving of 7.3 % instead of a battery around 1 100 kWh with a fuel saving of only 6 %, is a delayed startup of the second genset. As Fig. 13 shows, the genset power is relatively smooth compared to the power load, and the battery covers the difference. When the ramping price was reduced, the battery stopped contributing in some of these active periods. The battery usage being this sensitive to the ramping price suggests that some effort should be put into finding estimates for this parameter which to a larger degree is based on real costs.

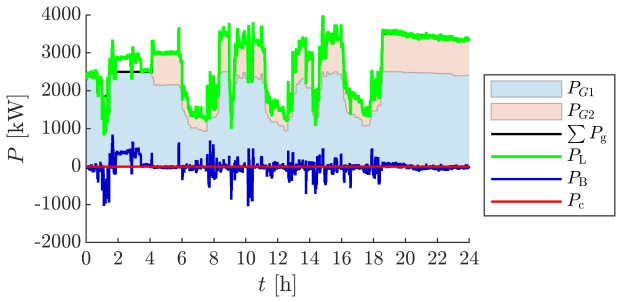

Figure 13: Power balance for a system with a battery capacity of 1 500 kWh, only including started gensets.

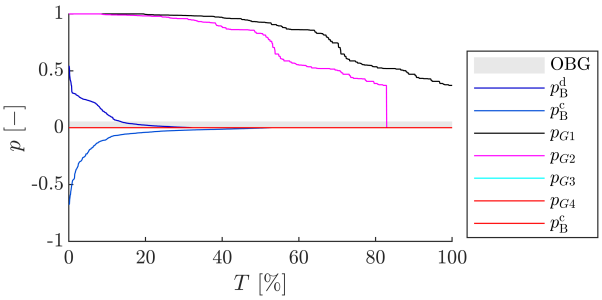

Figure 14: Duration curves per unit per component for a system with a battery capacity of 1 500 kWh.

One should, arguably, be careful basing a system design solely on such a small amount of data. In the included data, this vessel had only short periods where the load was relatively low. The small engines are, thus, not started in most cases. For data series with longer time periods with low load, the second smallest genset might be increased in capacity in order to avoid running the large gensets in these periods.

The power utilization of each component can be read from the duration curves in Fig. 14, which shows that the battery power loading rarely is over 50 %, and that most of the battery power is not utilized. The lowest genset loading under operation is 37 %. Testing different battery sizes showed that the number of hours at high part-load is increased significantly when the large single genset is replaced in operation by the smaller gensets.

Fig. 15 shows the baseline power distribution of each started genset together with their fuel curve. The distribution is presented as genset hours relative to the optimization horizion. By comparison with Fig. 16, it is apparent that the solver chooses to run the gensets at a higher relative loading a larger share of the time. Two of the gensets are running at 90–100 % loading a large portion of the time.

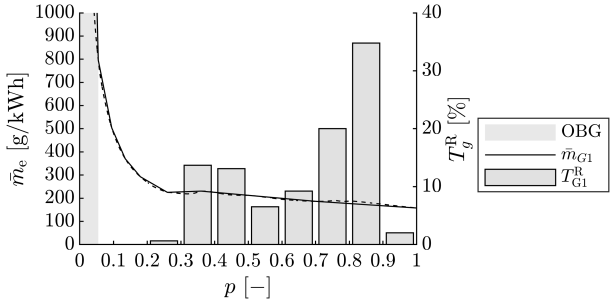

Figure 15: Genset loading for the existing system without a battery.

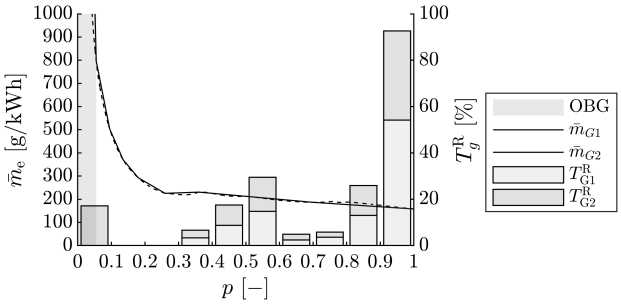

Figure 16: Genset loading for a system with a battery capacity of 1 500 kWh.

The state of charge of the battery is presented in Fig. 17. From comparing this SoC with the power balance in Fig. 13, it is apparent that the solver considers it optimal to increase the SoC when possible, in particular initially, and uses this accumulated energy to postpone the startup of the second genset. The limitation is here on the energy capacity of the battery,

which is drained down to the minimum allowed SoC. At this point the second genset was started and used to both cover the increased load and to recharge the battery. This can be seen from the power balance in Fig. 13, and is even more clear from the SoC presented in Fig. 17.

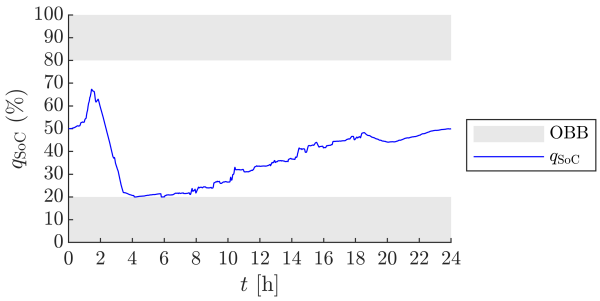

Figure 17: Battery SoC for a system with a battery capacity of 1 500 kWh.

3.5 Further Discussion

There are some aspects and implications of the results which should be highlighted through further discussion. These are addressed in the following paragraphs.

3.5.1 Energy Storage System

It is essential not to overlook weaknesses in the method, as they might lead to the design of systems that are unusable in real applications. For one, more effort needs to be put into finding which maximum C-rate to use, depending on the time resolution of the optimization problem. Using the same C-rate can result in power system configurations which becomes infeasible when the resolution is increased. Scaling the C-rate with the time resolution will enable the full utilization of energy capacity by covering a larger share of the slower, large power variations. However, such scaling should take into account how much the power fluctuations are smoothed by the reduction in time resolution to ensure that sufficient battery power is available for to cover fast power fluctuations, rather than scaling it proportionally with the time resolution itself.

It could further be considered to implement a varying maximum C-rate based on the local power variation of the second-data around the mean values, in order to take into account that the battery should be able to cover these fast power fluctuations. This could prove difficult to implement in the MILP approach, but could be included in more detailed system simulations. It should also be taken into account which usage of the battery is desired: backup storage only, delaying of genset startup, helping out for fast ramping of gensets and/or peak-shaving fast power fluctuations.

3.5.2 Power Generation Systems

One weakness of using low time resolution data, is usage in combination with allowing the gensets to run at 100 % loading over time, where they cannot – or should not – serve the short-term power variations which exceed the average maximum power value over time. This increases the need for having a sufficiently large battery capacity available to cover the power fluctuations around that power output.

Expansion with Other Technologies: In future work it could be of interest to expand the model with more components and energy domains. Most trawlers today have fuel-mechanic propulsion due to the propulsion being one of the larger consumers in both power and energy. Adding the mechanic connection could for this reason be interesting for the industry.

The algorithm is flexible for implementation of alternative energy technologies, where alternative fuel curves and fuel parameters can be used to define different technologies. A natural next step here could be to include and investigate systems powered by battery together with other internal combustion technologies fuelled by e.g. liquefied natural/bio gas (LNG/LBG), or dual-fuels with methanol or ammonia. Fuel cells would also be interesting to include for some applications. Furthermore, large ships like container vessels and offshore service vessels might consider nuclear-fuelled systems in the future which makes expanding the model with nuclear reactors combined with thermal storages and steam turbines something that could be considered relevant for future work. This would make the approach more generic and flexible for the solutions that might come to market over the upcoming years. The economic feasibility of installing reactors on trawlers might be considered limited. However, it would be interesting to evaluate. Furthermore, the tool should be flexible to implement for other vessel segments as well, where nuclear systems could be considered more feasible.

In order to evaluate an alternative fuel, one would need the same presented parameters and fuel curves presented in Tab. 1, for each of the technologies of interest, and a power load from a comparable vessel.

The approach is currently limited to loading-dependent costs linked to the fuel consumption. This is a bit limiting considering that running the engines/gensets on different loads can increase costs for other reasons too. In future work, it might be pertinent to consider the part-load maintenance costs. Running the gensets on low load can lead to sooting and over

time increased maintenance costs. On the other hand, running the gensets long periods at close to full loading can over time increase the wear and tear which further increases the maintenance needs. Replacing the part-load fuel curve with a part-load cost curve could be a natural next step, which include cost for any desired behaviour. In other words, include more details in the existing linearized PWA model instead of expanding the model, in order to not increase the size of the optimization problem. This could, however, increase the need for more discretization points and if so, this increase should be considered against alternative implementation approaches.

3.5.3 Model Resolution, Precision and Computational Effort

The solver time proved a challenge in some cases. Running an analysis with a long load time series together and many components with both high time resolution and high resolution of the linearized fuel consumption and degradation curves in the optimization might not be realistic. This is the case for both the initial genset configuration design stage and in the later battery sizing and analysis stage. Some steps should be taken to evaluate which parts of the input models and data can be simplified while keeping the integrity of the results, with the goal of scaling up the manageable scope of investigation.

The running time of the analysis increases significantly for large systems. Most of this time was, however, spent building the model and not for solving for the optimal solution. This despite the model size being reduced by lowering the resolution. This could suggest that the current problem-based optimization formulation is a major limitation when wanting to scale up the size of the analysis. Some further effort could be put into implementing the approach using a solver-based optimization formulation to see if this could reduce the heavy computational effort of the analysis.

3.5.4 Application for Energy System Design

As previously mentioned, the tool is built to be flexible in several ways. Flexible in terms of included technologies and level of detail, but also flexible in terms of application. Depending on the input and implementation of the tool, different levels of analysis can be conducted and different parties can have use of it.

One application is to run the presented genset configuration and battery sizing application as a static analysis, for instance conducted by a ship designer. At first, low-resolution data and models can be used to make a rough draft of the energy system. A range of different scenarios and components can be investigated in order to find a roughly suitable one for the specific needs of the vessel. After running the preliminary analysis, high-resolution data and models can be used to investigate the theoretically optimal utilization of the chosen system. This usage and performance is not necessarily realistic to achieve during operation due to limited knowledge of future load fluctuations, but can still give valuable insight into how the system should be sized and utilized in different situations.

3.5.5 Choice of Available Gensets

A large contribution to the increasing computational effort is the high number of parameters per each new genset included. It is, thus, important to carefully choose which components to include. It is crucial which size ranges are included, but also which combinations of sizes are available to choose from. It might, for example, be cheaper and more practical to have two of the same size instead of only including unique genset sizes. This might be more sensible from a maintenance perspective as well, making it more manageable to have spare parts available.

Starting the genset configuration stage without a strategic approach to what to investigate might, for this reason not be a good option. Instead of starting from scratch, it could be more practical to start with a set of genset sizes found the more traditional way, and then investigate the savings potential from changing only some of them at the time.

Too much freedom could also, potentially, result in impractical system configurations. The output should for this reason always be evaluated and considered for additional constraining or shaping of the optimization problem. It could be a good approach to run the optimization problem several times with not only different battery sizes but also different specific gensets, iteratively. Instead of letting the algorithm choose to install smaller gensets and run them all at once, since this increases the fuel consumption. Or, alternatively, to lock one large genset to be installed. For example, could the optimization be run to size single components when being replaced, in order to find a more suitable size considering the expected load in retrofit projects, e.g. by constraining some of the MG and the AG's to be installed, and only let gensets in the LG size be available for picking.

This might be the most sensible when using traditional fuels. However, if later introducing alternative fuels, it might become necessary to start from scratch and keep more size options open. At least in situations where experience of what are the reasonable component sizes is not available.

3.5.6 Data Selection - Reference Data Set

Due to the fast-growing size of the optimization problem when including extra components, only a small subset of the gathered power measurements are included in this analysis. The remaining data set shows large variations in power demand and component utilization, and it was observed that the results from the optimization are heavily dependent on the selected time period. The included 24 hours are not necessarily enough to conclude on the overall optimal energy system configuration and emissions reduction potential of the vessel. However, the results show some of the underlying mechanisms in the tool and some expected results if the data can be considered representative.

When using such a tool to design a system, it is therefore crucial to include a load series which is representative of the lifetime usage of the vessel. One weakness with the method is the necessity of finding that representative load data. However, an increasing number of vessels have equipment for onboard continuous data logging which can be gathered and used to make a reference data set for the ship designers can use. This should be looked into further. For trawlers, this reference data set could consist of time series for the propeller power demand and for the electric power demand.

The reference data set needs to fulfil some requirements in order to be considered representative. It needs to a) take into account the whole utilized power range b) include all the relevant operating modes, c) take into account a realistic distribution between each mode and d) take into account the typical order in which the operating modes typically occur. Alternatively, the reference data set could be generated from simulations of the expected operation.

3.5.7 Evaluation of Results and Future Studies

The usage of the suggested optimization approach to genset and battery sizing should be done with caution and the behaviour of the output needs to be evaluated before investing. For one, the output from the optimization could be run through a high-resolution time-domain simulation with a PMS/EMS system to investigate the feasibility of the suggested system and how much the system performance can be improved. In particular, investigations of how the high-frequency power fluctuations impact the instantaneous power balance could be considered to evaluate if the installed battery size and C-rate is sufficient. A desired operational mode-based SoC profile could, for example, be included to let the battery try and operate close to optimal. Looking into this further is a natural next step.

Some input parameters might need to be adjusted in order to get the desired behaviour when the load input varies in a different pattern, and additional constraints might need to be included in order to remove other unwanted behaviour which has not been uncovered or addressed in this work.

Another next step could be to apply the tool on data from different vessels and analyse how other ship segments can benefit from a cost-optimization based approach to system configuration design and utilization.

3.5.8 Application for PMS/EMS Design

Potentially one of the more valuable outputs from such an optimization-based analysis is information about which gensets are reasonable to start and have running at different times, based on different operational modes, and which state of charge to approach in order to be ready for realistic load variations for the current and planned operational modes. This general experience can be used to design and tune the vessel's PMS/EMS, more than necessarily using the instantaneous power values from the optimization output themselves in a real-time system.

The optimal analysis can be used to find the desired state of charge during different operational modes in order to be ready for the probable load variations. The tool could be used to investigate this specifically, and the experience from the output can be used to make the control algorithm for the battery. Here, high resolution historic data could be used.

3.5.9 Application to Decision Support System

Another application is to use as a on-board user decision support system during operations. This would require the operator to input the expected operations over the upcoming period. This might be challenging, since the transition between the operational modes largely are dependent on external factors.

The results from the presented work suggest that the largest emissions reductions during operation can be achieved by delaying the starting of the second genset by discharging the battery temporarily. Having available a tool for the ship operator to use a prediction of the future load conditions to schedule the future power demand would, thus, be of high value. However, although it might be unrealistic for a vessel's operator to have detailed knowledge of the future power load, knowledge that postponing the startup of a genset might reduce the fuel consumption in general load-increasing situations is easy to implement in a real scenario without a state of the art support system.

On the other hand, during operation the crew has some knowledge about their plan for upcoming activities over the next few hours. Although this is impacted

by weather, as well as found fish and catch per haul, they do have a rough idea of future activities. This information could be combined with experience from the optimization as to how the system should be operated. This could be used during operations in a way where the captain defines the planned activities over the next hours which could auto-generate an estimated future load profile based on historic data, which could in return give the captain suggestions on which gensets to start or stop, and the power control unit information on how to use the battery.

Increasing the time resolution significantly is interesting when the goal is to find out the result from optimal usage of the system, but is not realistic in practice. Future load is hard to predict with a high degree of certainty, especially with a high time resolution, although different statistical methods and machine learning could be applied to create reasonable scenarios based on the operational mode and values from the last time steps. Automated or manual on-board decision support systems could possibly contribute here to generate a rough prediction some time ahead. The application is for this reason important when choosing a time resolution.

4 Conclusion

In this study, a MILP-based optimization approach for selecting a genset configuration and battery size is proposed and applied on measurements from an existing trawler. The approach takes into account part-time fuel efficiency of gensets modeled from gathered data as PSFC-curves, and battery degradation using a model from the literature. It has been demonstrated that the optimization framework can suggest a sufficiently redundant genset configuration where the number of startups and engine hours can be limited at the same time as reducing the fuel consumption.

The results show that the optimization tool can be used as proposed to find a reasonable genset configuration and battery capacity to achieve a cost-efficient fuel-reduction. With the included limited power load time series, fuel savings of 7.3 % can be achieved in a cost-efficient manner, through a combination of better sizing of installed gensets and postponing starting installed gensets enabled by dispatching battery power. If using the existing genset configuration, the results imply that it is not cost-efficient to install a battery. However, by applying the optimization approach described in this article on the gathered data under the requirement of installing the same number of gensets, an alternative system is proposed for the given trawler, with installed genset power capacity $P_g^{\mathrm{N}} \in \{2\,500,\ 1\,000,\ 350,\ 326\}$ kW and a battery with installed energy capacity of 1 500 kWh.

The results suggest that a sufficiently large battery can enable two things: 1) cover the peak power demand which reduces the necessary capacity of both installed and running gensets, and 2) temporarily store energy to run installed gensets at a more fuel-optimal loading. However, this is only if the battery has large enough both energy capacity and power capacity. If the battery is not large enough, a larger genset needs to be installed and run, at which point it is not necessarily cost-efficient to use the battery for peak-shaving.

A reduction in time resolution to 5 minutes appears to be a viable choice to limit the solver time. The reduction in model size gives more value to the analysis by enabling the inclusion of a higher number of components, than the seemingly small and predictable variations in the results and the loss in precision reduces its value. The ramping price should be kept low in order to avoid unnecessarily steady genset loading with associated frequent curtailment of produced power.

Further effort should be put into calculating values for the maximum battery C-rate depending on the chosen time resolution and genset ramping price, as well as options to further limit the maximum allowed genset ramp rate without increasing the curtailed power. Alternative technologies like dual-fuel systems using ammonia, methanol or LNG should also be included in further model expansions and case studies.

Acknowledgements

The authors of this article want to thank SINTEF Ocean for providing raw measurement data from the energy system of a fishing vessel.

References

Bunker, S. . World bunker prices. 2024. URL https://shipandbunker.com/prices. [Accessed: 28.05.2024].

Chapaloglou, S., Nesiadis, A., Iliadis, P., Atsonios, K., Nikolopoulos, N., Grammelis, P., Yiakopoulos, C., Antoniadis, I., and Kakaras, E. Smart energy management algorithm for load smoothing and peak shaving based on load forecasting of an island's power system. *Applied energy*, 2019. 238:627–642. doi:10.1016/j.apenergy.2019.01.102. Publisher: Elsevier Ltd.

Chapaloglou, S., Varagnolo, D., Marra, F., and Tedeschi, E. Data-informed scenario generation for statistically stable energy storage sizing in isolated power systems. *Journal of energy storage*, 2022.

51:104311–. doi:10.1016/j.est.2022.104311. Publisher: Elsevier Ltd.

Duggal, I. and Venkatesh, B. Short-term scheduling of thermal generators and battery storage with depth of discharge-based cost model. *IEEE transactions on power systems*, 2015. 30(4):2110–2118. doi:10.1109/TPWRS.2014.2352333. Place: PISCATAWAY Publisher: IEEE.

Enova. Enova gir støtte til utviklingen av miljøvennlig sjøtransport. 2024. URL https://www.enova.no/bedrift/sjotransport/.

European Commission. Food-based dietary guidelines recommendations for fish | knowledge for policy. 2024. URL https://knowledge4policy.ec.europa.eu/health-promotion-knowledge-gateway/food-based-dietary-guidelines-europe-table-9_en.

Fortenbacher, P., Mathieu, J. L., and Andersson, G. Modeling and optimal operation of distributed battery storage in low voltage grids. *IEEE transactions on power systems*, 2017. 32(6):4340–4350. doi:10.1109/TPWRS.2017.2682339. Place: PISCATAWAY Publisher: IEEE.

Hennum, T. Data-driven stochastic model predictive control of an isolated microgrid. 2021. URL https://ntnuopen.ntnu.no/ntnu-xmlui/handle/11250/2828784.

Hennum, T., Kjerstad, Ø., Nerheim, A. R., Skjong, S., and Ladstein, J. A modeling and simulation based assessment of switching fuels for a norwegian fishing vessel. In *Proceedings of the 37th ECMS International Conference on Modelling and Simulation*. pages 394–400, 2023. doi:10.7148/2023-0394.

Marocco, P., Ferrero, D., Martelli, E., Santarelli, M., and Lanzini, A. An MILP approach for the optimal design of renewable battery-hydrogen energy systems for off-grid insular communities. *Energy conversion and management*, 2021. 245:114564–. doi:10.1016/j.enconman.2021.114564. Place: Oxford Publisher: Elsevier Ltd.

Norges Fiskarlag. Utslipp skal halveres. 2020. URL https://fiskarlaget.no/utslipp-skal-halveres/.

Norwegian Directorate of Fisheries. Fartøyregisteret. 2024. URL https://www.fiskeridir.no/Yrkesfiske/Registre-og-skjema/Fartoeyregisteret/fartoyregisteret.

Norwegian Directorate of Health. Kostrådene. 2024. URL https://www.helsedirektoratet.no/faglige-rad/kostradene-og-naeringsstoffer/kostrad-for-befolkningen.

Norwegian Seafood Council. Why norwegian wild-caught seafood is sustainable. 2020. URL https://en.seafood.no/sustainability-articles/why-norwegian-seafood-is-sustainable/.

Skjong, E., Johansen, T. A., Molinas Cabrera, M. M., and Sørensen, A. J. Approaches to economic energy management in diesel-electric marine vessels. *IEEE Transactions on Transportation Electrification*, 2017. doi:10.1109/TTE.2017.2648178. Accepted: 2017-09-01T12:58:07Z Publisher: IEEE.

Sustainable Ships. Cost overview - batteries. 2024. URL https://www.sustainable-ships.org/key-insights/costs-batteries. [Accessed: 19.05.2024].

United Nations. Agriculture technology for sustainable development: leaving no one behind. 2021.

Vieira, G. T., Pereira, D. F., Taheri, S. I., Khan, K. S., Salles, M. B., Guerrero, J. M., and Carmo, B. S. Optimized configuration of diesel engine-fuel cell-battery hybrid power systems in a platform supply vessel to reduce CO2 emissions. *Energies (Basel)*, 2022. 15(6):2184–. doi:10.3390/en15062184.

Wang, Y., Zhou, Z., Botterud, A., Zhang, K., and Ding, Q. Stochastic coordinated operation of wind and battery energy storage system considering battery degradation. *Journal of modern power systems and clean energy*, 2016. 4(4):581–592. doi:10.1007/s40565-016-0238-z. Place: Berlin/Heidelberg, Publisher: Springer Berlin Heidelberg.

Æsøy, L., Piehl, H., and Nerheim, A. R. System simulation-based feasibility and performance study of alternative fuel concepts for aquaculture wellboats. In *Proceedings of the 41st ASME International Conference on Ocean - OMAE2022*. American Society of Mechanical Engineers, 2022. doi:10.1115/OMAE2022-81106. Book Title: Volume 4: Ocean Space Utilization.